

Chapter 1: Introduction

a) The Cape fur seal, general considerations and rationale behind the study

Three families comprise the group of carnivores commonly known as the pinnipedia. These are the Otariidae (fur seals and sea lions), the Phocidae (true seals) and the Odobenidae, the walrus, comprising a single genus *Odobenus*. In the family Otariidae, nine species of fur seal exist, eight of which belong to the genus *Arctocephalus* and a single species, the Northern fur seal, belonging to the genus *Callorhinus*.

The South African (Cape) fur seal *Arctocephalus pusillus pusillus* is the only pinniped endemic to southern African waters (Oosthuizen 1991) and breeds on and feeds off the South African south coast and the west coast of South Africa and Namibia (Fig. 1). In this range, seals are commonly found as far north as the non-breeding colony of Cape Frio in Namibia (18°S 12°E), and as far east as Black Rocks (34°S 26°E) on the South African south coast (Wickens *et al.* 1991). In this area, they breed and feed at 25 breeding colonies (19 of which are situated on islands and six on the mainland) while a further nine non-breeding colonies (as defined by having no, or minimal and erratic pup production (Oosthuizen & David 1988)) are presently known to exist (Oosthuizen 1991).

Distribution of the Cape fur seal throughout this range is uneven, with some 5% of the total found along the South African south coast, 60% along

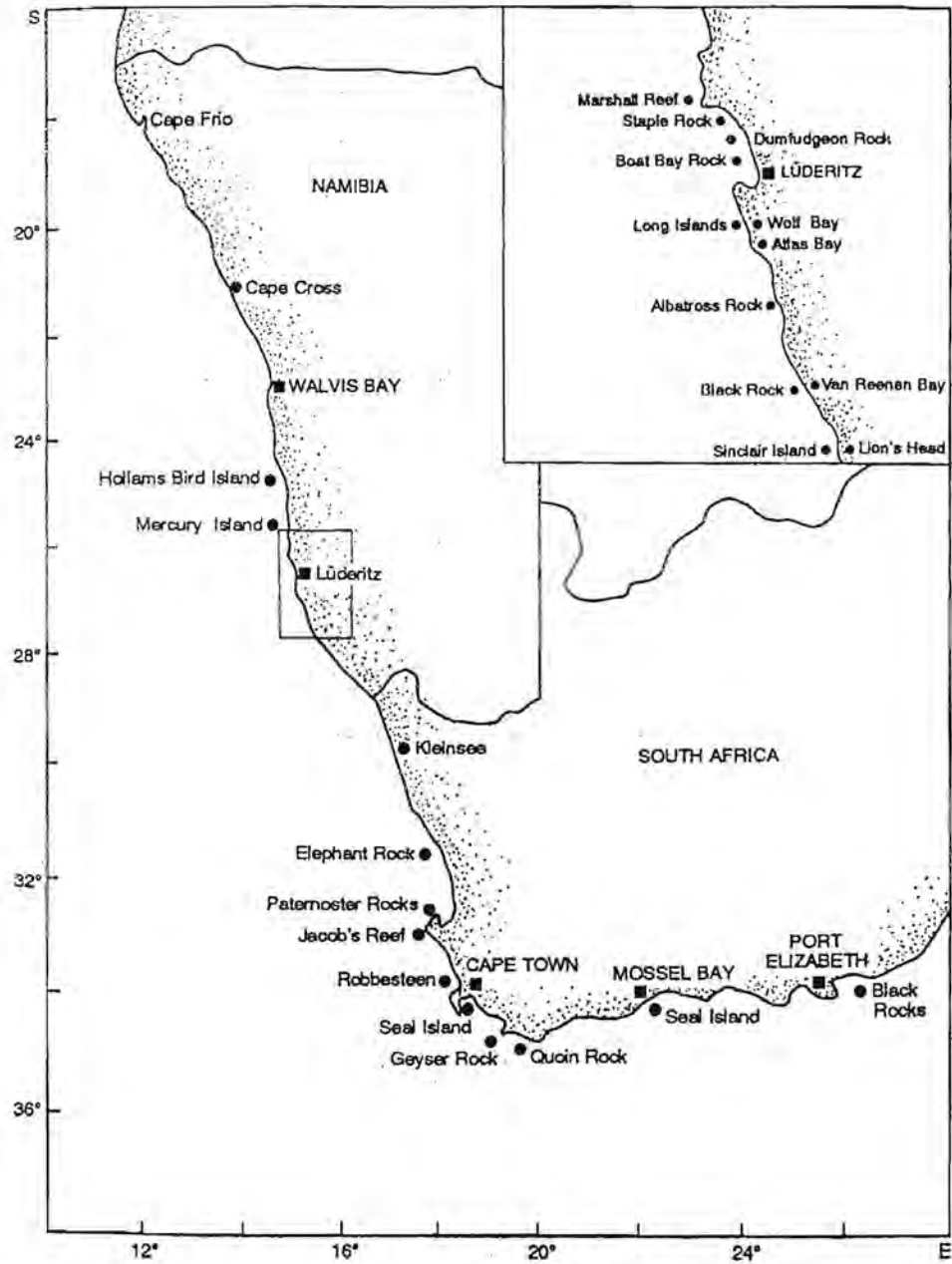


Fig. 1: Map of southern Africa, showing the distribution of the Cape fur seal

the Namibian coast, and 35% inhabiting the South African west coast (Miller *et al.* 1996). It is an abundant animal, currently estimated to number some two million individuals (Butterworth *et al.* 1995), which makes the Cape fur seal one of the three most abundant fur seal species in the world (Wickens & York 1997), and is estimated to be increasing at some 3% annually (Butterworth *et al.* 1995). The Cape fur seal is a coastal, non-migratory animal, generally foraging over the coastal shelf and occurring not more than 220 km offshore, although substantial movement within their range may take place (Oosthuizen 1991). Occasional vagrants may be found far outside their normal range, even as far afield as Marion island (48°54'S 37°45'E), some 2000 km from Cape Town (Kerley 1983).

The west coast where the Cape fur seal is most abundant is an area with an extremely high productivity (David 1987a), which, as a result, is also an area that sustains a profitable fishing industry (Wickens *et al.* 1992). Since some two thirds of Cape fur seal prey species consist of commercially important fish (Butterworth 1992, Butterworth *et al.* 1995), this overlapping between seal range and fishing area results in a high incidence of interaction between seals and fishery operations. These include both biological interactions (e.g. seals taking fish directly from fishing operations, resulting in lost catches and fears that an artificially high seal population is supported by the fisheries industry) and operational interactions (such as fishing gear being damaged, or fish shoals being dispersed), as discussed

by Wickens *et al.* (1992) and Wickens (1994). Such interactions, coupled to the continued increase in the seal population, and the suspension of seal culling in 1990 (in South Africa, at least) have led to fears that fishery catches may decline as a result of seal predation.

Fishermen in particular are vocal in this regard, believing seals to be major competitors, understandably so, since seals consume an estimated 2 million tons of food annually (Butterworth *et al.* 1995) even though David (1987a) believes that the role of seals as competitors may have been overemphasized due to their being disproportionately conspicuous animals. Furthermore, estimates by Wickens *et al.* 1992 suggest that losses to fisheries because of seals may be relatively insignificant, at least as far as operational interactions are concerned, though the issue of biological interactions remains more controversial. Nevertheless, information on whether a reduction in seal numbers, whether by culling or harvesting, will in fact aid the fisheries industry is equivocal (Butterworth *et al.* 1988, Butterworth 1992) and there is no unequivocal evidence that seal culling or harvesting will lead to improved fisheries catches (Butterworth 1992, Wickens 1995), since the extra fisheries resources which would then become available would likely be exploited by other predators (such as hake *Merluccius capensis*) rather than fisheries.

Successfully addressing this complex management issue requires improved knowledge of specific aspects of the biology, population dynamics and interspecific interactions of the Cape fur seal.

The histology of reproduction and a general description of the reproductive cycle has been done for the male (Stewardson *et al.* 1998) as well as the female Cape fur seal (Rand 1955), though the latter study was done in the absence of an accurate ageing technique. Vital population parameters, such as age of puberty, age of sexual maturity, age specific fecundity rates and age- and sex-specific survival rates require a reliable way of assigning ages to seals. In the absence of an intensive mark-recapture program, it is only recently that such a technique has become available (Oosthuizen 1995, 1997), allowing a description of the reproductive cycle of the Cape fur seal, assessing morphology and determining the retention / persistence of ovarian structures.

Reproduction in pinnipeds has been studied in numerous species, Enders *et al.* (1946) and Pearson & Enders (1951) paving the way with their work on the Northern fur seal *Callorhinus ursinus*, followed by a detailed description of the reproductive tract in *C. ursinus* by Craig (1964) and a summary of reproductive habits by Harrison (1969). Pinnipedian reproduction has been found to display great similarity in pattern, both between and within species. All pinnipeds, for example, have a seasonal reproductive cycle with synchronous parturition during a restricted, often short breeding season (e.g. 90% of Cape fur seal births have been found to occur within a 34-day period (Shaughnessy 1979) with some variation between geographical areas, David (1987b) reporting 90% of births to occur within a 26-day period at van Reenen Bay. Parturition is followed by a short

post-partum oestrus which may occur at variable times after pupping, ranging from 3-5 days in *C. ursinus* (Craig 1964, Daniel 1981), 6-10 days in the subantarctic fur seal, *Arctocephalus tropicalis* (Bester 1995), or roughly one week in the Cape fur seal (Rand 1955). In phocids, this may be somewhat longer, e.g. 14-18 days in the grey seal *Halichoerus grypus* (Boness & James 1979).

Successful mating is followed by a period of delayed implantation, followed by implantation and gestation to give a total duration of pregnancy of roughly one year (Daniel 1981), although exceptions in this do occur, such as e.g. the walrus, *Odobenus rosmarus* (Harrison 1969) and the Australian sea lion, *Neophoca cinerea* (Tedman 1991) in which the reproductive cycle may continue for a second year (or part thereof as in the Australian sea lion). Pinnipeds tend to be mono-oestrus (Harrison 1969, Boyd 1991b) and a single ovum is usually released each year, ovulation generally occurring from the ovary contralateral to the uterine horn of recent pregnancy (e.g. Craig 1964, Pearson & Enders 1951, Rand 1955).

b) The mammalian oestrus cycle, origin and fate of the *corpus luteum*

A short description of the general mammalian oestrus cycle follows. Information for this chapter, which has also been used as an aid throughout the present study, has been obtained especially from Stevens & Lowe

(1992) and Wheater *et al.* (1995) with additional information obtained from sources as quoted where relevant.

In the mature ovary, undeveloped follicles exist as primordial follicles, consisting of a primary oocyte, surrounded by a single layer of follicular cells. Enlargement of the oocyte, coupled to the enlargement of the follicular cells (now referred to as granulosa cells), results in a primary follicle. A homogeneous glycoprotein layer between the oocyte and the granulosa cells is now formed, referred to as the *zona pellucida*. Concentric layers of stromal cells surround the follicle, giving rise to an organised layer of cells called the *theca folliculi*, separated from the granulosa cells by a basement membrane.

Few follicles develop past this stage, becoming atretic. Follicles that do become secondary follicles, have granulosa cell layers increasing in thickness and the *theca folliculi* differentiating into two layers, the inner *theca interna* (responsible for secreting oestrogens) and the outer layer, the *theca externa*, which probably has no secretory function. Accumulation of follicular fluid between the cells of the *zona granulosa* gives rise to a small, fluid filled gap, enlarging to form a large, fluid filled cavity, the follicular antrum, the formation of which results in the follicle being termed tertiary, or Graafian (Craig 1964). The formation of the antrum results in the granulosa layer being pressed into a thin layer of equal thickness around the periphery of the follicle excepting only one area, the *cumulus oophorus*, where the granulosa layer is still thickened, and to which the oocyte is attached.

Reduction of the *cumulus oophorus* leaves the mature oocyte surrounded by the *corona radiata*, projecting into the antrum, but still attached to the granulosa layer by a thin bridge of cells. Most follicles become atretic before reaching this stage, follicular atresia being evidenced by the formation of a glassy membrane of dense hyaline between the *membrana granulosa* and the *theca interna* (Craig 1964). This results in a structure called a *corpus atreticum* (CAT), and which may eventually be replaced entirely by collagenous tissue.

Usually one (but on occasion two or rarely more, in monotocous species) follicle ruptures during ovulation, and the follicular fluid, together with the oocyte is released into the *tuba uterina*. Bleeding from the follicular wall into the antrum, especially from the *theca interna*, may follow ovulation and a small blood clot may form inside the collapsed follicle. Luteinizing hormone, secreted by the anterior pituitary, causes the granulosa cells to luteinize, a process involving hypertrophy and being filled with a yellow pigment, lutein. Cells from the *theca interna* may also be luteinized and contribute to the functional *corpus luteum* (Craig 1964, Ouelette & Ronald 1985, Laws & Sinha 1993 and Iwasa & Atkinson 1997) although they may be less important and not always easy to distinguish from granulosa lutein cells (Ouelette & Ronald 1985).

Luteal regression after, or even prior to parturition, entails two processes, pyknosis and vacuolization, the former entailing the regression of the nucleus while the latter is evidenced by the formation of vacuoles in the

cytoplasm (Pike *et al.* 1960, Craig 1964). Regression of the luteal cells in this manner, coupled to luteal cell loss, gradually causes a reduction in the progesterone secretory activity of the gland. Invasion of luteal tissue by macrophages, neutrophils, fibroblasts and connective tissue completes the process, and the *corpus luteum* eventually appears as a small white scar, consisting entirely of collagenous tissue, the persistence of which may vary between species (Laws & Sinha 1993).

At this stage the small *corpus albicans* may sometimes be confused with the *corpus atreticum* referred to above and may require histological methods to be distinguished from it (chapter 3, results). Gradual merging with the surrounding ovarian stroma gradually renders the *corpus albicans* invisible, and it disappears.

Chapter 2: Materials and Methods

2.1 Sample size and origin of study material

The present study examined the reproductive organs of female Cape fur seals ($n = 159$) which had been killed during various months of the year. The reproductive organs were obtained primarily from an existing collection of samples, accumulated by the Chief Directorate, Marine and Coastal Management (formerly the Sea Fisheries Research Institute, SFRI), Department of Environmental Affairs and Tourism. These samples were obtained from animals killed during routine field trips to breeding rookeries between 34°S , 26°E and 18°S , 12°E since 1974, as well as during routine SFRI research cruises along the west coast of South Africa and Namibia, especially for the purposes of dietary studies (as described in David 1987a). Details of relevant collection cruises are summarised in Table 1.

A number of samples ($n = 128$) was selected from this collection, selection being conducted randomly as far as possible, although two criteria nevertheless influenced the selection process.

Firstly, research cruises / visits conducted by the (then) SFRI, were not evenly distributed throughout the year, with the result that the various months of the year were not all represented equally in terms of available samples. This problem was addressed to some extent in that available material was supplemented by samples from a further 31 females collected during 1997/1998,

Table 1: Summary of collection trips during which samples had been collected at sea

Month	Dates of collection	Place of collection	ID numbers of animals collected	Distance offshore (miles)
Jan	12-22/01/1988	Cape Town to Buchu twins	3803 - 3853	1.1 - 18
	15-19/01/1990	Cape Town to Lamberts Bay	4161 - 4226	3 - 41
Feb	13-16/02/1989	Cape Town to Lamberts Bay	3898 - 3915	0.7 - 35
Mch	8-27/03/1979	Cape Cross (Möwe Bay)	946 & 950	2 - 27
	26-30/03/1990	Cape Town to Lamberts Bay	4411 - 4459	4 - 42
Apr	12-15/04/1988	Cape Town to Lamberts Bay	3645 - 3706	0.5 - 33
	10-13/04/1989	Cape Town to Lamberts Bay	3958 - 3994	2 - 14
May	8-18/05/1986	St. Helena Bay to Walvis Bay	3209 - 3297	1 - 37
Jun	1995	Kleinzee breeding colony	5026 - 5106	0
July	13-25/07/1987	Walvis Bay to Kunene River	3458 & 3483	1 - 15
Aug	28/08-01/09/89	Cape Town to Lamberts Bay	4051 - 4082	4.2 - 41
Oct	16-20/10/1989	Cape Town to Lamberts Bay	4093 - 4154	1.6 - 48
Nov	1985	Kleinzee breeding colony	2944 - 3144	0
Various months	1997/98	Kleinzee breeding colony	5128-5158; APP5-APP9	0

at especially the Kleinzee breeding colony by MCM technicians during routine field trips. Monthly sample sizes finally ranged from none for September, to thirty for November. Secondly, the age determination of the animals was, and still is an ongoing process, not directly related to the present study, and large numbers of females remain to be aged. Females of known ages were therefore selected over females of unknown age. Of the total sample of 159 females, only 83 had been aged to date, and were therefore available for the calculation of age-specific reproductive attributes (such as age at puberty or age at sexual maturity). The reproductive tracts from the remaining 76 females were examined primarily for seasonal variation in reproductive characteristics.

2.2 Age determination

Technical personnel attached to the SFRI / MCM was, and is, responsible for the process of assigning ages to animals. Age determination was performed as described by Oosthuizen (1995, 1997). Teeth were ground sectioned, and age determination effected by the counting of dentinal growth layer groups (GLGs). Canine pulp cavities in the Cape fur seal close upon reaching 13 years of age (Oosthuizen 1995, 1997), and hence all animals older than 13 years were grouped in a single age class, and given a single arbitrary age of 13+. The female Cape fur seal may have a potential longevity of over 20 years, perhaps even exceeding 30 years (Wickens 1993). A large and widely disparate group of animals may therefore have been included in this single age class, and will

remain so as Oosthuizen (1995, 1997) reports that cemental GLGs, which can be used as an alternative to dentinal GLGs in assigning ages to animals over 13 years, are unsatisfactory in terms of accuracy.

2.3 Tissue processing

The methodology by which reproductive tracts were examined has been performed successfully by a number of authors (e.g. Tedman 1991, Bester 1995), as summarized by Laws & Sinha (1993).

All ovaries were removed from the fixative (10% formalin) and weighed with an electronic scale to the nearest 0.1 gram. Three linear dimensions (length, width and height) were measured to the nearest 0.01 mm. The three measurements were then averaged to produce an average ovarian diameter, which was used as an index of ovarian size.

Following this, a few ovaries were - as a trial - embedded in a cornmeal-gelatin matrix as described by Pimlott & Mossman (1949), after which they were sectioned with a hand held blade into sections of about 3 mm. Ovaries were sliced serially along the longitudinal axis in such a manner that each slice retained its attachment to the ovary at the broad ligament. This allowed the sequential study of each slice without the slices losing their relationship to each other. Use of such a gelatin matrix was discontinued however, since the absence of such a matrix did not seem to impact negatively on the sectioning efficiency, and saved on time and effort in pre-processing the ovaries. All ovaries were

subsequently sectioned as described above, directly upon removal from the fixative.

2.4 Macroscopic ovarian examination: *corpora lutea* / *corpora albicantia*.

The surface of each ovarian slice was examined sequentially for the presence or absence of *corpora lutea* (CLs) or *corpora albicantia* (CAs). Where present, the three linear dimensions of each of these structures were measured, and averaged to produce an average corpus diameter, which was then used as an indication of CL or CA size.

First *corpora albicantia* (1st CAs) were defined for the purposes of this study as those CAs found in the ovary contralateral to that containing the active *corpus luteum* (in other words, which were active *corpora lutea* in the previous reproductive cycle). Exceptions, such as where double ovulations have produced double *corpora albicantia* are specifically mentioned where relevant.

Similarly, second *corpora albicantia* (2nd CAs) are those structures resulting from active CLs from two reproductive cycles earlier and are generally found in the ovary containing a newly formed CL. Third and even fourth CAs have been recorded (as noted in Appendix 1) but no CA older than a second CA later than July/August (i.e. roughly 30-32 months post-ovulation) was used in any back-calculations in this study, except where specifically mentioned. Older structures were disregarded for the simple reasons that their incidence and sizes seemed to have become increasingly variable between individuals, and their

overall small sizes made them increasingly difficult to distinguish macroscopically from *corpora atretica*.

2.5 Follicular cycle

In each ovary, the numbers of visible (i.e. roughly 1mm or larger in diameter) Graafian, or tertiary follicles (as evidenced by the presence of an antrum) were counted. In each ovary, two visible, linear dimensions (the longest diameter, and one perpendicular to it) of the largest follicle were measured and averaged to produce an index of follicular size. Small Graafian follicles, invisible due to their being smaller than the average thickness of each ovarian slice could be identified clearly by holding each slice up to light, and counting follicles otherwise missed. Occasionally, where only small follicles were present inside the ovary, ovarian slices had to be sliced once more, so as to expose follicles in order to measure them.

2.6 Microscopic ovarian examination

Female reproductive organs were collected by different researchers / technicians, at different times, and with different purposes in mind. The result was that the way in which reproductive organs (and ovaries in particular) were stored or treated was not always standardized. Certain logistical constraints resulted in many ovaries being frozen upon collection, and which were only

thawed and transferred to 10% formalin at a later stage. Others were immediately placed in 10% formalin. When freezing tissue, various microscopic changes take place in the tissue - such as cells rupturing, resulting in the leakage of cell fluid, and the distortion of cell size and shape (M vd Merwe, University of Pretoria, pers. comm.). This reduces the value of such tissue for histological purposes, and many samples could therefore not be examined histologically.

Ovaries from 46 females - all of which were fixed in formalin without prior freezing, and thus free of the detrimental effects of such treatment - were used in a microscopic examination of ovarian structures. Slices containing relevant, or interesting ovarian features were dehydrated, cleared (with xylol) and embedded in paraffin wax using standard histological techniques. Slices were sectioned at 7 μm , mounted on slides, stained with Haematoxylin and counterstained with Eosin. In no case was the entire ovary sectioned.

In each CL or CA, the length and width of 25 luteal cells were measured to the nearest 0.01 μm with an eyepiece micrometer, and the two measurements averaged to produce an average diameter, referred to throughout the text as cell size. This was coupled with a qualitative description of the appearance, persistence and changes in these structures at different times of the reproductive cycle.

2.7 Macroscopic examination of the uterine horn

In addition to the ovaries, a small piece of both uterine horns was also available for examination in most (n = 119) females. This sample often consisted of a piece of uterine mucosa of no more than roughly 1-2 cm² in surface area. No samples of uterine horn from the remaining 40 females were available.

Based on an examination of the available material, females were classified as being nulliparous, primiparous or multiparous as defined by Pike *et al.* (1960). A nulliparous female is a female with two non-parous uterine horns (in other words, a female which is not bearing, and has never born a conceptus in either uterine horn). A primiparous female has one parous horn (and is thus bearing, or has born a young in one horn), while a multiparous female shows evidence of bearing, or having born young in both horns.

A non-parous horn has a thin and smooth muscle layer, and the mucosa is thin, with low, narrow and closely apposing rugae. A parous horn has a thickened and distorted muscle layer and the mucosa is thickened, with thick, enlarged rugae which do not closely appose each other. The implantation site of the blastocyst was used as a more important uterine characteristic by which the recent reproductive history of a female could be determined. The placental scarring in the uterine horn resulting from this appears as a locally disrupted, orange-brown discoloured section of the endometrium (as described by Pearson & Enders (1951)), and referred to as a zonary band, or ZB (e.g. Bester 1995).

The presence of a zonary band in a uterine horn was assumed to be a certain indication of implantation (and hence successful mating and conception) to have taken place. The converse - namely that the absence of such a structure implies no implantation to have taken place - was not assumed, and the presence of a zonary band was on occasion inferred based on the macroscopic and microscopic appearance of the CL or CA, as compared to corpora of animals killed at the same time of year in which pregnancies had been confirmed.

This unfortunate assumption was deemed necessary, based on the fact that uterine material was unavailable for a large number of females, and that uterine samples that were available were sometimes inadequate for ascertaining with confidence the incidence of blastocyst implantation, either because of the small size of the sample, or the area from which the uterine sample had been collected. Only in three cases did the accompanying data sheets refer to uterine scars where none was visible on the available material, and in these three cases the presence of zonary bands was assumed to be valid.

Additionally, obvious placental scarring may not be an inevitable result of pregnancy, since it is possible for implantation and subsequent pregnancy to occur without readily detectable concomitant placental scarring, as reported by Pearson & Enders (1951) for the Northern fur seal (*C. ursinus*) and Bester (1995) for the Subantarctic fur seal (*A. tropicalis*). CL/CA appearance and placental scarring were therefore not used in isolation of each other in determining current or recent reproductive history, and each was used, as far as possible, as a

confirmation of the other. This technique brings an unfortunate yet inevitable degree of subjectivity into the reproductive study, and inferring pregnancy may possibly have resulted in an underestimation of the incidence of reproductive failure, with reference to the November sample in particular.

2.8 Age of puberty/age of sexual maturity

The age of puberty was defined as the age at which reproduction first becomes possible, as determined by the presence of *corpora lutea*, *corpora albicantia* or mature follicles.

The age of sexual maturity has been variously defined in the past as the average age at which conception first takes place (e.g. Laws & Sinha 1993, Bester 1995), the average age at first implantation, irrespective of whether or not the pregnancy is then taken to term (Craig 1964), or the age at which ovulation commences (as evidenced by the presence of CL, CA or mature follicles (Hewer 1964, McLaren & Smith 1985, Bjørge 1992, Andersen *et al.* 1999). For the purposes of this study, the age of sexual maturity has been taken as the age of first implantation, irrespective of whether the pregnancy was then taken to term, or underwent premature termination

Several different ways exist whereby the age at puberty or the age at sexual maturity in marine mammals can be calculated, not all equally accurate (DeMaster 1984). The average ages of puberty and of sexual maturity were calculated in this study following the technique described in DeMaster (1978).

According to this, the average age of puberty (or sexual maturity, if the former is replaced by the latter in the following formulae, and “ovulating” by “implanting”) can be calculated as follows:

$$f(x) = t(x)/n(x)$$

$$P(x) = f(x) - f(x-1)$$

$$\chi = \sum_{x=1}^{\omega} (x)P(x)$$

where $f(x)$ = the estimated probability of ovulating at or before age x

$t(x)$ = number of females in sample of age x who have ovulated

$n(x)$ = the number of females in sample of age x

$P(x)$ = estimated probability of first ovulating at age x

χ = average age of puberty

ω = maximum age in sample (taken as 8 years after back-calculating, as described below)

In ageing animals, the ages were rounded off to the closest birthday (which was taken as December 1 (Oosthuizen 1995, 1997)). Therefore, in back-calculating to first conception or ovulation, the ages of animals during the previous reproductive cycle were used if they were collected during the first half of the reproductive cycle (up to and including May), but for animals collected after May, their ages from two years back were used. In the case of pre-pubertal animals (which had not begun ovulating, or showed no apparent signs of approaching

first ovulation, such as maturing follicles), the ages at the time of being collected were used.

2.9 Pregnancy rates

Pregnancy rates were calculated in three ways. In the first, pregnancy rates were calculated for the previous reproductive cycle, using the presence / absence of zony bands in conjunction with the presence/absence of CAs (Referred to in the results as birth rates). November animals were excluded from this estimate, due to the lack of uterine material for this month, and the variability in CA sizes and appearance at that late stage.

Secondly, pregnancy rates were calculated for the current reproductive cycle, using the presence/absence of an embryo or foetus as a guide or, where absent, using the presence/absence of a functional CL, its appearance, and evidence of recent placental scarring as indicators of pregnancy. Pre-implantation animals (January to April samples) were excluded from this estimate.

Thirdly, the age specific pregnancy rates were calculated for the total sample of 83 known-age females. For this purpose, the reproductive status during the reproductive cycle during which the females had been collected was used, except in the case of females in the pre-implantation stage, where back-calculations to the previous year were made. Small sample sizes for certain age classes made this a less than satisfactory exercise, and for this reason, all

animals older than eight years, but younger than 13+ were included in a single age group for the purposes of this calculation. The 13+ year group was not included in this group, for examining this group separately allowed the presence of senescence, or an age-specific reduction in fertility rates in older females, to be identified.

2.10 Statistical analyses

Samples and means were compared - where relevant, to each other using the *t*-test for independent samples. Correlations between samples or variables were measured using regression analyses, or, when more than one variable was to be grouped and compared to another, multiple regression was used. In all cases was the standard deviation used, except in calculating the numbers and sizes of follicles (results, section 3.2) where the standard error of the mean was used. The calculations were done using the Statistica (Microsoft) (Windows 1995) software program while the background concepts and formulae were obtained from Fowler & Cohen (1992).

Chapter 3: Results

3.1 Ovarian weight and size

The ovarian weight cycle is shown in Table 2 and is depicted graphically in Fig. 2. The CL-ovary shows a gradual increase in weight, from a low at the end of the breeding season in January (9.73 ± 2.06 g), to a maximum weight during August (14.42 ± 5.85 g). After August, the weight once more declines towards the following breeding season in November and December. The pre-implantation pregnant ovary (January, up to and including March) has a significantly lower weight than that of the implantation and post-implantation ovary (April to December) ($t = 4.60$, $df = 153$, $p = 0.000009$). This trend in ovarian weight closely resembles that of ovarian size (Table 2, Fig.3).

Ovarian size (in pregnant females) shows an increase between the end of the breeding season, from a low during January (24.60 ± 1.90 mm), reaching a peak during August (28.65 ± 5.74 mm), with ovarian size decreasing afterwards, as the CL starts decreasing in size (described in section 3.3). A significant difference between the pre- and post-implantation ovarian sizes exists ($t = 4.20$, $df = 153$, $p = 0.000046$). These fluctuations in size and weight are clearly correlated primarily with the luteal cycle. A significant correlation exists between the CL size and both the ovarian weight ($R = 0.63$, $F = 97.35$, $df = 1,149$, $p < 0.0004$) and ovarian size ($R = 0.62$, $F = 92.31$, $df = 1,149$, $p < 0.00001$). This correlation is enhanced only slightly when performing a multivariate regression,

Fig. 2: Ovarian weights (g) of ovaries with CLs and with CAs respectively (bars indicateSD)

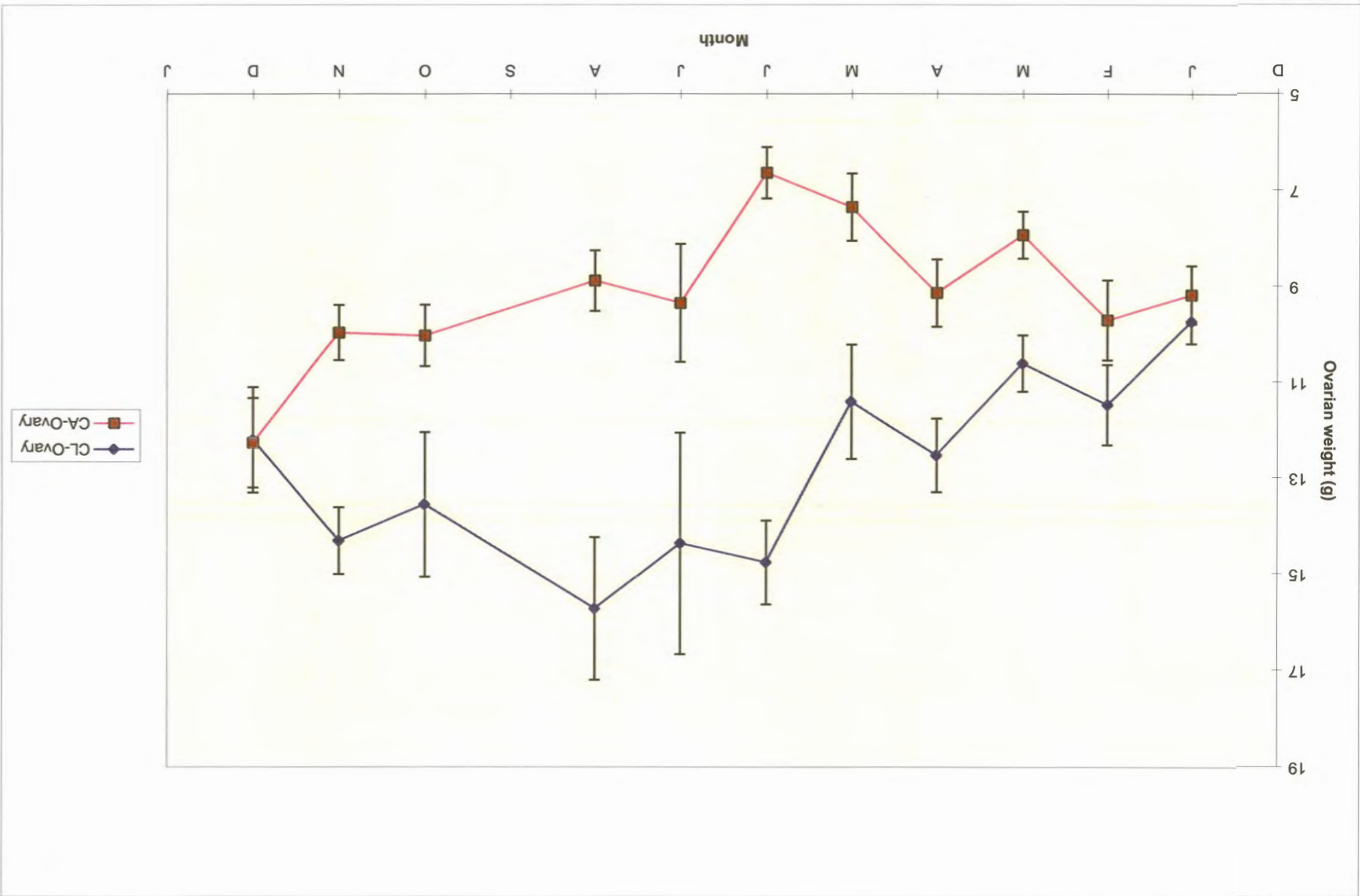


Fig. 3: Ovarian sizes (mm) of ovaries with CLs and with CAs respectively (bars indicate SD)

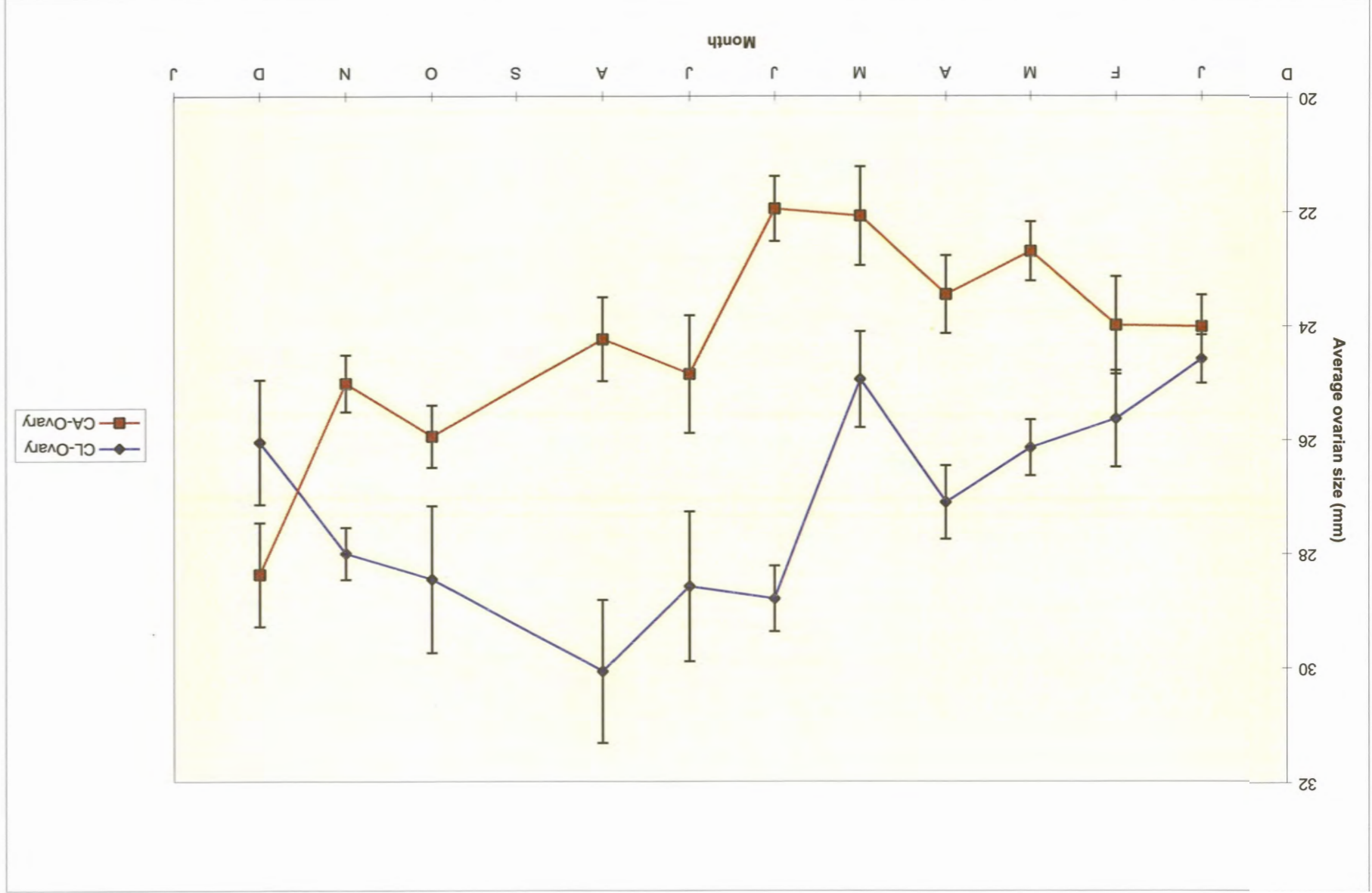


Table 2: Average monthly ovarian sizes (mm) and weights (g), \pm standard deviation

	CL-Ovary (size)	CL-Ovary (weight)	CA-Ovary (size)	CA-Ovary (weight)
Jan (n=20)	24.60 \pm 1.90	9.73 \pm 2.06	24.03 \pm 2.49	9.17 \pm 2.71
Feb (n=6)	25.65 \pm 2.08	11.47 \pm 2.05	24.01 \pm 2.10	9.70 \pm 2.05
Mch (n=19)	26.16 \pm 2.15	10.60 \pm 2.56	22.71 \pm 2.26	7.93 \pm 2.12
Apr (n=15)	25.97 \pm 4.09	11.56 \pm 3.88	22.90 \pm 3.01	8.52 \pm 3.08
May (n=11)	23.94 \pm 3.74	10.19 \pm 4.35	21.60 \pm 3.31	6.92 \pm 2.38
Jun (n=15)	28.81 \pm 2.23	14.75 \pm 3.38	21.97 \pm 2.20	6.63 \pm 2.06
Jul (n=7)	28.59 \pm 3.47	14.36 \pm 6.10	24.87 \pm 2.74	9.34 \pm 3.25
Aug (n=9)	28.65 \pm 5.74	14.42 \pm 5.85	23.45 \pm 3.29	8.25 \pm 2.67
Sep	-	-	-	-
Oct (n=15)	28.34 \pm 4.87	13.28 \pm 5.83	25.50 \pm 2.31	9.66 \pm 2.46
Nov (n=30)	28.02 \pm 2.50	14.30 \pm 3.81	25.03 \pm 2.72	9.96 \pm 3.15
Dec (n=5)	26.06 \pm 2.45	12.20 \pm 2.46	28.39 \pm 2.04	12.26 \pm 2.09

correlating CL-size and follicular numbers together with ovarian weight ($R = 0.63$, $F = 49.69$, $df = 2.148$, $p < 0.0197$).

The contralateral ovary, containing the regressing CL (now termed the CA) shows a dissimilar picture, fluctuating both in size and weight, but showing an initial slight and gradual downward trend, reaching a minimum weight of 6.63 ± 2.06 g and size of 14.75 ± 3.38 mm (Table 2, Figs. 2 & 3) in June, which constitutes a significant drop from the weight and size during January when the breeding season ended ($t = 2.56$, $df = 33$, $p = 0.054$ and $t = 3.025$, $df = 33$, $p = 0.00478$ respectively). Thereafter, both size and weight begin to increase once more, most likely because follicular activity at this time is on the increase (as described in results, section 3.2). The factors affecting the changes in the CA-Ovary size and weight are apparently less definite, both the size and weight showing a poor correlation with either follicle numbers ($R = 0.31$, $F = 15.82$, $df = 1,150$, $p = 0.000108$ and $R = 0.18$, $F = 5.13$, $df = 1,150$, $p < 0.0000$), or with CA-diameter combined with follicle numbers ($R = 0.36$, $F = 9.46$, $df = 1,124$, $p = 0.000150$ and $R = 0.23$, $F = 3.55$, $df = 1.124$, $p = 0.0315$).

Throughout the entire reproductive cycle, the ovary containing the CL remains significantly heavier ($t = 9.44$, $df = 302$, $p = 0.000001$) and larger ($t = 9.02$, $df = 302$, $p = 0.000001$) than the CA-ovary and it is only during December, during the peak of the breeding season that the latter approaches or exceeds the former in these attributes. This may be due to the large number of follicles, (averaging 32 ± 10.08 (SE), the largest follicles in December averaging 5.41 ± 0.73 mm, inside the CA-ovary (section 3.2).

Seven immature animals were found in the collection, the data of which have been excluded from Table 2 and Figs. 2 & 3. Their ages range from 3 years (n = 4) through 4 and 5 years (n = 1 each) to one female aged 7 years. No significant differences were found between the left and right ovaries of these animals either as for size ($t = 0.028$, $df = 12$, $p = 0.98$) or for weight ($t = 0.39$, $df = 12$, $p = 0.70$).

3.2) Follicular cycle

In the ovary with an active corpus luteum, follicle numbers were at a maximum at the end of the breeding season, numbering 55 in female 4225 and 65 in female 5012. Most of these, however, were atretic. The follicle numbers continued to increase marginally towards March, after which they showed a marked drop during April (Fig. 4). This trend is also seen in Fig. 5 where the average diameter of the largest follicle in the CL-ovary increases sharply towards March and April. Follicles approach, even exceed 10 mm during this period. One female, (APP9), had 55 Graaffian follicles in March the largest of which had an average diameter of 10.77 mm. This period of peak follicle activity is followed by a sudden drop both in follicle numbers and sizes, most of those remaining presumably becoming atretic soon afterwards. This becomes evident during the months following implantation as the *corpus luteum* becomes presumably reactivated, and luteal suppression of follicle activity becomes marked. The follicle activity in the CL-ovary continues to drop, reaching a minimum during December, at the peak of the following breeding season. At this stage, follicle numbers range from

Table 3: Follicular sizes (mm) and numbers, \pm standard error of the mean.

	CL-ovary numbers	CL-ovary diameter	CA-ovary numbers	CA-ovary diameter
Jan (n=20)	18.70 \pm 3.75	3.38 \pm 0.37	3.85 \pm 1.49	1.35 \pm 0.31
Feb (n=6)	21.00 \pm 4.75	4.51 \pm 0.34	5.83 \pm 3.98	2.88 \pm 1.07
Mch (n=19)	21.84 \pm 2.97	7.05 \pm 0.64	13.42 \pm 2.32	4.80 \pm 0.46
Apr (n=15)	14.33 \pm 1.78	5.52 \pm 0.50	11.93 \pm 2.34	5.55 \pm 0.56
May (n=11)	6.45 \pm 1.91	5.00 \pm 0.62	7.09 \pm 1.89	3.71 \pm 0.69
Jun (n=15)	6.13 \pm 1.07	3.37 \pm 0.51	16.73 \pm 2.58	4.45 \pm 0.45
Jul (n=7)	13.14 \pm 2.69	5.13 \pm 1.00	9.29 \pm 2.67	4.46 \pm 0.93
Aug (n=9)	4.44 \pm 1.83	2.61 \pm 0.67	13.67 \pm 3.75	3.81 \pm 0.62
Sep	-	-	-	-
Oct (n=15)	2.33 \pm 0.93	1.54 \pm 0.55	16.07 \pm 2.57	4.19 \pm 0.68
Nov (n=30)	3.77 \pm 0.94	2.31 \pm 0.52	22.97 \pm 2.79	5.61 \pm 0.39
Dec (n=5)	3.40 \pm 1.78	1.10 \pm 0.45	32.00 \pm 10.08	5.41 \pm 0.73

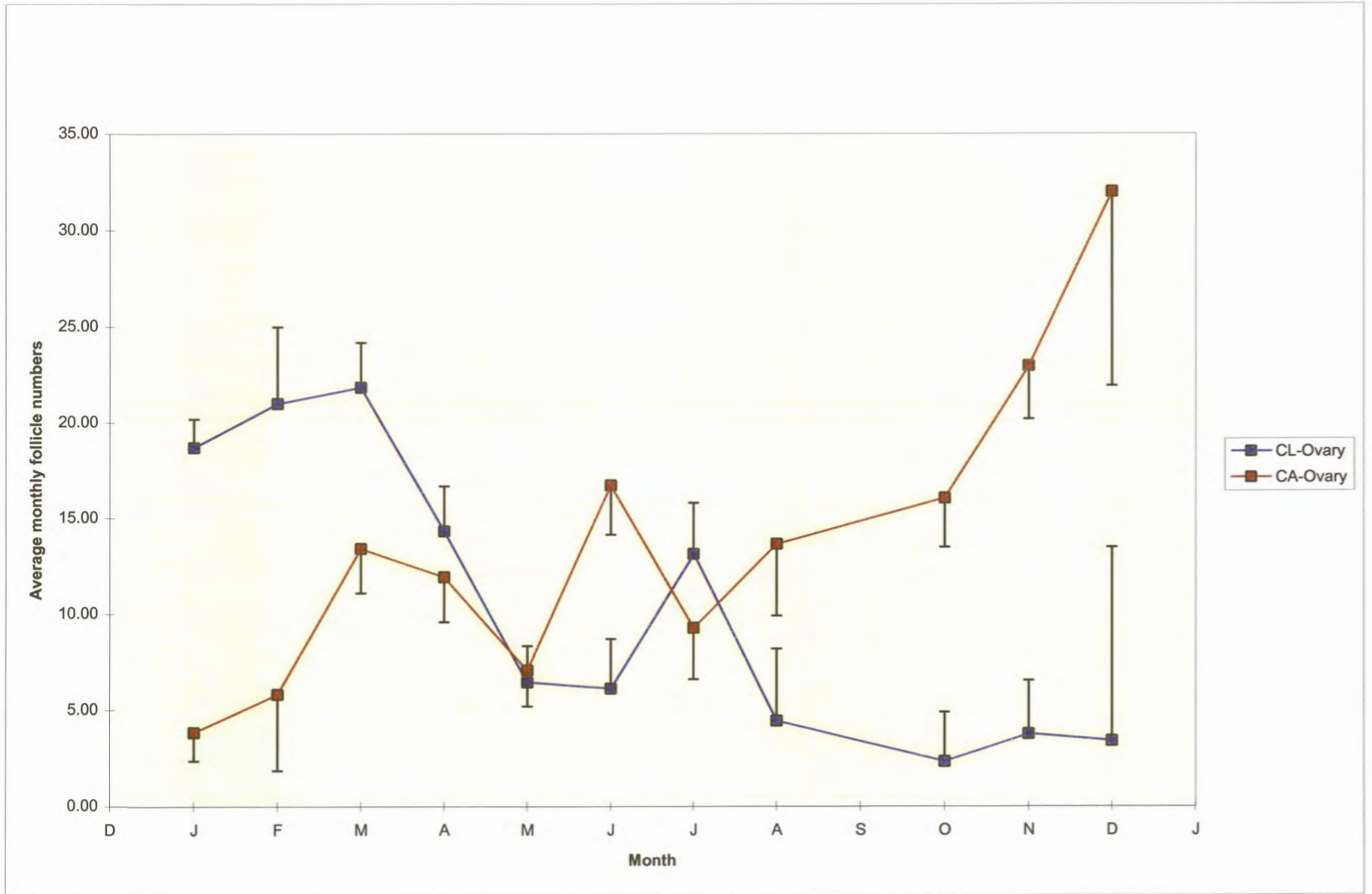


Fig. 4: Average monthly numbers of Graafian follicles, in ovaries with a CL and a CA respectively (bars indicate SE)

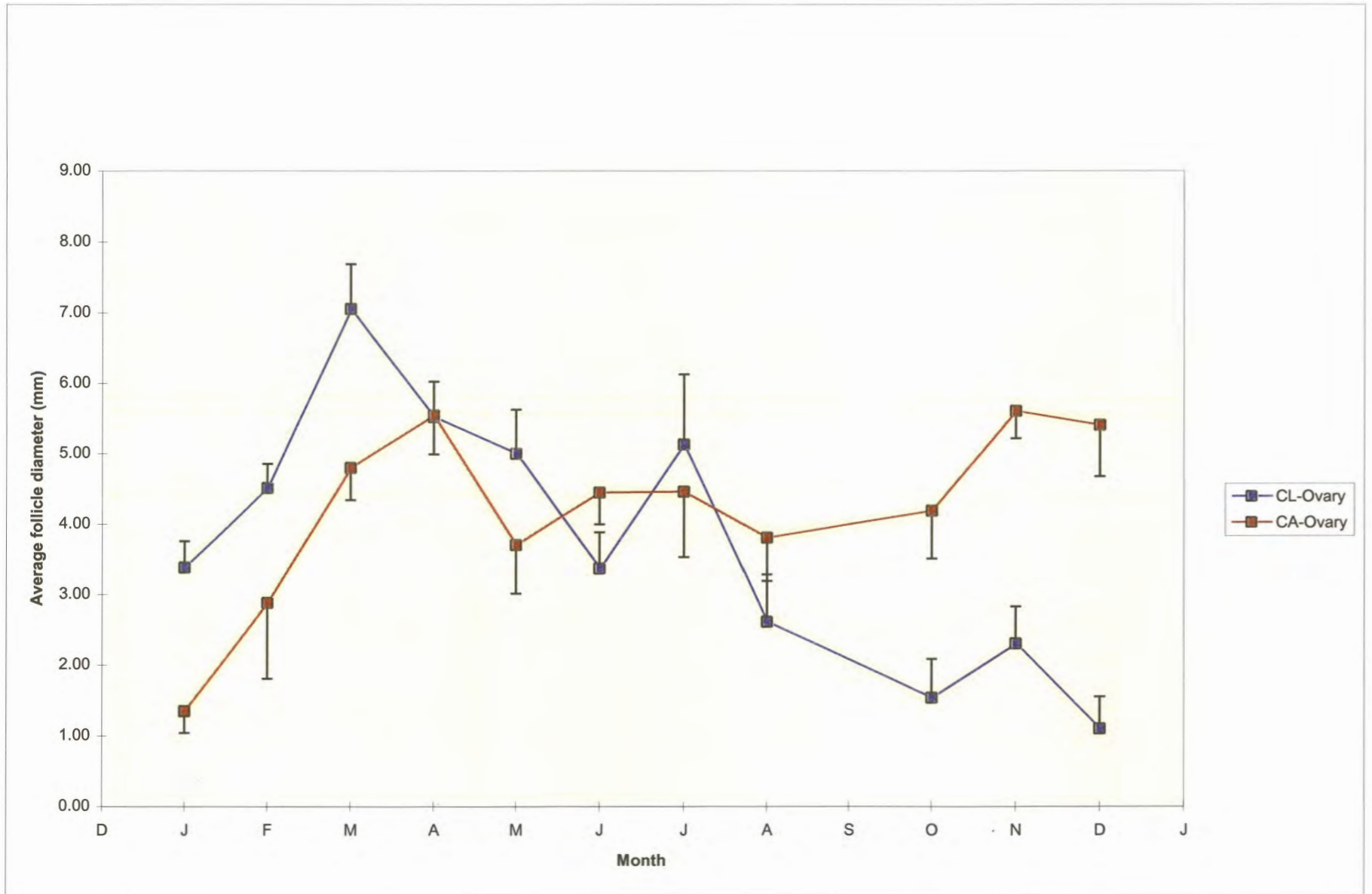


Fig. 5: Average monthly maximum follicular sizes in ovaries with CLs and CAs respectively (bars indicate SE)

0 to 9, all of them smaller than 2 mm.

The above trend is roughly reversed in the contralateral ovary, where the follicle activity initially increases from a minimum at the end of the breeding season when follicle suppression by the resorbing CL still seems to continue, with follicle numbers ranging from 0 to 5, mostly under 2 mm in size, during January. Exceptions exist, though, in ovaries which had had no CL during the previous breeding season, or had suffered an interrupted pregnancy. In these ovaries, follicular numbers range up to 23, although they tend to be relatively small and presumably atretic for the most part, but histological confirmation of this was not possible in all of these ovaries.

In all ovaries, follicle activity increases towards implantation, though not to such a large extent as occurs in the ovary with a young CL.

Following implantation, follicle activity in the CA-Ovary diminishes, but does not disappear. Follicle numbers fluctuate without a clear trend in size or numbers, follicles that are formed seemingly becoming atretic before maturing. *Corpora atretica* of the type shown in Figs. 6 & 7, the remnants of atretic follicles, appear to be common in both ovaries throughout the year, but especially so during the period between June and August. While no actual counts were made, they appear to number in dozens per ovary, although few of these are large enough to be visible with the naked eye. Those that were visible, however, appeared as small white scars of dense connective tissue, similar in appearance to a small CA. It is only towards the end of autumn that follicle activity increases once more. Between August and October, a gradual increase seems to be taking

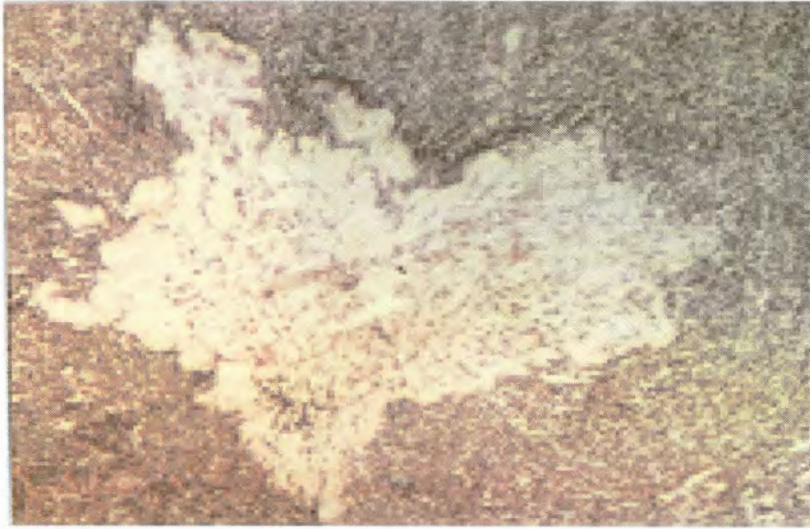


Figure 6: *Corpus atreticum* in a female (5157) of unknown age, collected during January (80 x)

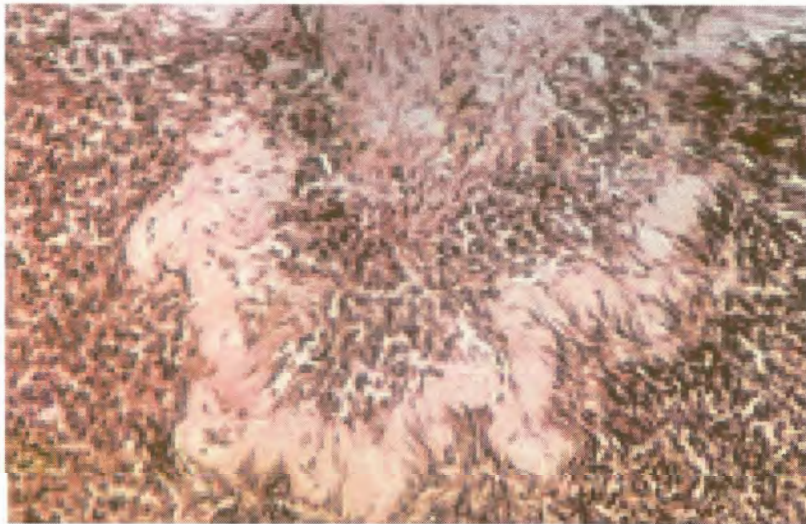


Figure 7: *Corpus atreticum* in a female (5012) of unknown age, collected during December (200 x)

place, follicle numbers during August rising to as high as 32, and approaching 10 mm in size. During October, the first ovulations ($n = 5$) were observed, one of these thought to have occurred only days before (described in results, section 3.3).

After October, follicle activity, as evidenced by both numbers and largest sizes showed a large increase as the breeding season commenced in November, the average follicle number per ovary being 22.97 ± 2.79 (SE), individual females having as many as 64 follicles. Some females showed very little follicle activity during November, however, with 3 females having only three follicles, none of them mature. Two of these (females 2949 & 3144) do however have follicles between six and seven mm in size, both of them maturing.

Between the two peaks of follicle activity (autumn and spring), a third peak was noted during July, which may be related to a concomitant drop in CL size (results, section 3.3). Of the seven samples available for July, five were pregnant with a foetus in the uterine horn ipsilateral to the ovary with the CL. Two of these had follicle numbers of under ten ($n = 0$ and 7 respectively), the other three having between 10 and 20 follicles (females 5128, 5130 & 5131). The two remaining females (5129 and 5132) were both non-pregnant, yet showed signs of very recent terminations of pregnancy (neither had a foetus, but both had large, raw scars of placentation on the uterine mucosa, ipsilateral to the ovary with a CL).

3.3) Luteal cycle

The youngest *corpus luteum* observed was in female 5149 (of unknown age) which had ovulated during October, though showing a CA of abortion from the previous reproductive cycle (A ZB was present, but the CA was exceptionally small and resorbed). The ovulation had probably taken place very recently, possibly at most two or three days prior to the female having been killed, since the germinal epithelium had still not been repaired, and the antrum was in direct contact with the formalin fixative. All follicular fluid had presumably been washed away by the fixative, since no traces of blood could be seen within the antrum, as would have been expected following ovulation. No traces of a fine network of fibrin inside the antrum could be seen, which Rand (1955) observed inside a 4 day old *corpus haemorrhagicum* (CH). This CH was elongated, with the long axis perpendicular to the ovarian wall. It had an average diameter of 8.17 mm, and was excessively lobulated, due to the collapse of the follicle wall following ovulation. No apparent signs of luteinization, or of any sort of differentiation of thecal and granulosa cells could be observed.

A number of young CLs were observed between November and December. One from November (5154) and two from December (5008 & 5011) were examined histologically and were estimated to be about 3-4 weeks old. Another CL (5012) of a female killed during January had a CL very similar in appearance, possibly about a month old. This female in fact had two newly formed CLs, 11.41 and 10.53 mm in size respectively, which indicate a double

Table 4: Sizes of *corpora lutea* of pregnancy (mm) (abortions not included) \pm standard deviation.

	CL Graviditatis	CA (2nd year CL)	CA (3rd year CL)
Oct (new CL)	10.74 \pm 2.48 (n=5)		
Nov (new CL)	10.13 \pm 0.46 (n=3)		
Dec (new CL)	10.05 \pm 0.58 (n=3)		
Jan	12.28 \pm 1.66 (n=20)	13.00 \pm 1.47 (n=16)	4.38 \pm 2.10 (n=9)
Feb	12.96 \pm 1.62 (n=6)	13.15 \pm 2.36 (n=5)	3.61 \pm 1.34 (n=5)
Mch	14.91 \pm 1.54 (n=19)	10.29 \pm 2.25 (n=13)	4.05 \pm 2.08 (n=12)
Apr	16.78 \pm 1.79 (n=15)	12.26 \pm 2.12 (n=11)	3.27 \pm 0.61 (n=5)
May	17.50 \pm 2.17 (n=10)	11.56 \pm 1.82 (n=6)	2.55 \pm 1.36 (n=3)
Jun	21.97 \pm 2.42 (n=14)	9.75 \pm 1.06 (n=6)	2.68 (n=2)
Jul	18.88 \pm 4.83 (n=5)	10.47 \pm 0.88 (n=5)	2.87 \pm 0.93 (n=3)
Aug	22.28 \pm 3.38 (n=8)	8.78 \pm 1.84 (n=9)	3.83 \pm 1.68 (n=5)
Sep	no samples	No samples	no samples
Oct	19.46 \pm 4.97 (n=10)	8.51 \pm 1.80 (n=10)	
Nov	18.97 \pm 4.10 (n=26)	4.86 \pm 2.46 (n=24)	
Dec	16.14 \pm 2.12 (n=5)	6.61 \pm 4.35 (n=3)	

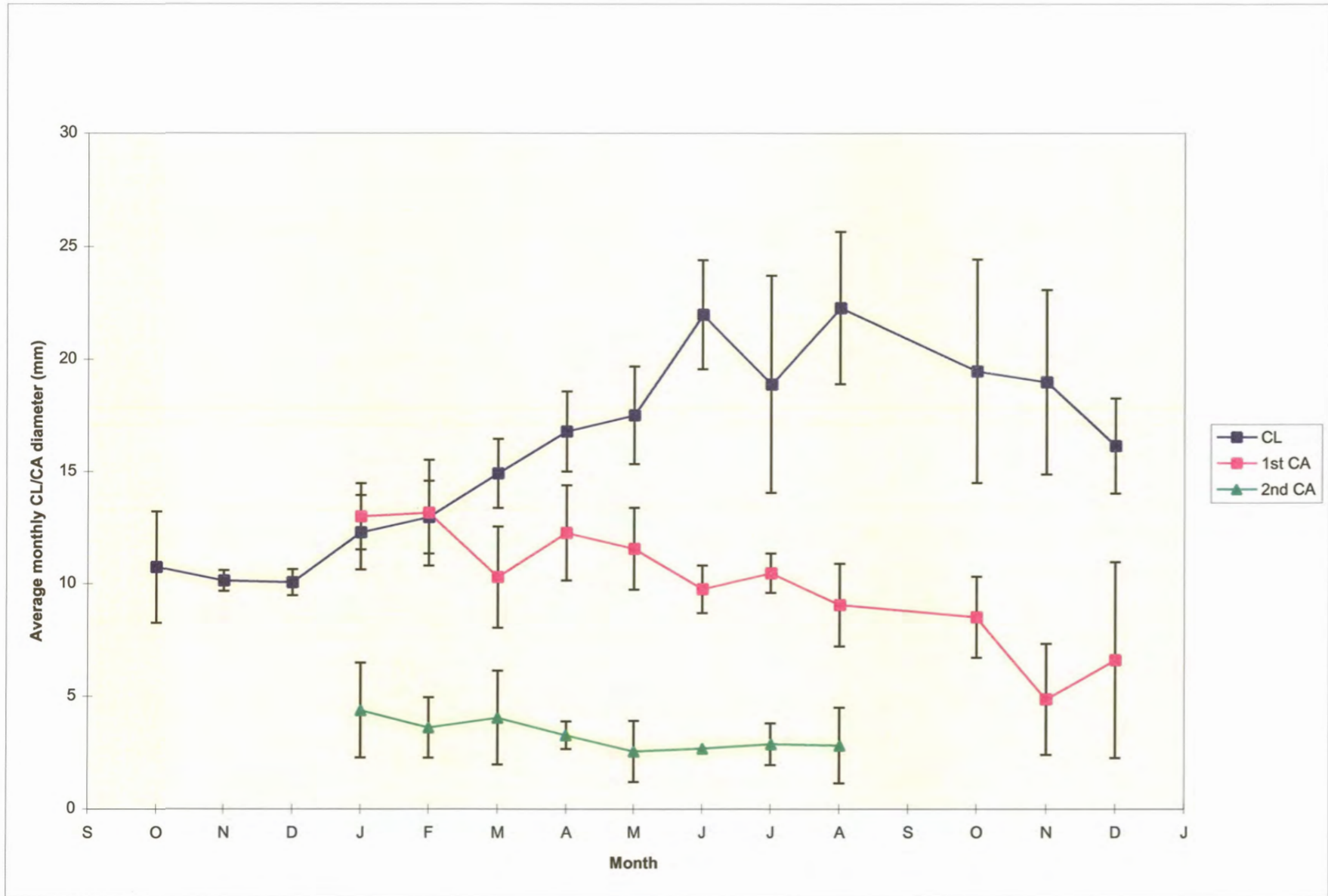


Fig. 8: The average monthly size of the CL/CA until 32 months after formation (bars indicate SD, except where sample < 3)

ovulation. The young, month-old CL is small, with an average diameter of about 10-11 mm (Table 4, Fig. 8). It is round or oval, but with a very lobulated appearance, due to the collapse of the follicular wall, which forms folds into what had been the antrum. This lumen itself seems to be filled with a jelly-like substance, presumably the remains of the *liquor folliculi*, mixed with blood and hardened by the fixative. It may be colourless, or may have a reddish colour. Upon microscopic examination, this central lumen was observed to contain loose blood cells as well as a loose network of fibrin.

The luteal cells at this stage are densely packed around the large central core, though do not occur homogeneously throughout the body of the gland. Large, fluid-filled gaps exist. These are spread throughout the body of the CL, interspersing large clumps of luteinized cells. The luteal cells are still small at this stage, ranging from 13.6 to 18.35 μm (Table 5, Fig. 9). They exist in two shapes or forms. Peripherally, the luteal cells have the more typical form, are round/oval, with large, central nuclei. The cell cytoplasm has a heterogenous, almost frothy appearance (Figs. 10 & 11). Deeper into the gland, closer to the central core, the cells are similar in average size, but have a much more elongated shape. In this area, the cells have a streaming appearance, as though radiating outwards from the central core. The heterogeneous appearance of the cytoplasm suggests that the cells are probably extremely active at this stage.

Histological material is lacking for February. The central core of the CL, however, is still very large, although the gelatinous blood clot has been replaced by dense connective tissue.

Table 5: Average luteal cell sizes (μm) \pm SD (average for each row is given in the final column)
 (Each box gives the ID number, L(ef) or R(ight) ovary, and type of structure).

Nov	2957R NCL 15.55 \pm 1.62	5154R NCL 18.35 \pm 2.14									16.95
Dec	4601L NCL 16.82 \pm 1.53	5011L NCL 19.04 \pm 1.50									17.93
Jan	5012R CL 13.60 \pm 1.88	5155L CL 16.83 \pm 1.00	5156R CL 23.34 \pm 1.84	5157L CL 13.53 \pm 1.86	5158R CL 16.69 \pm 2.41						16.80 \pm 3.99
Mch	AP5L CL 30.22 \pm 3.85	AP6L CL 31.34 \pm 4.30	AP7L CL 27.94 \pm 4.02	AP8R CL 31.29 \pm 4.05	AP9R CL 27.88 \pm 4.05						29.73 \pm 1.72
Jun	5039L CL 30.32 \pm 3.68	5087R CL 35.85 \pm 3.83	5090L CL 32.72 \pm 3.92	5095L CL 32.49 \pm 3.68	5096L CLA 34.65 \pm 4.24	5097R CL 32.73 \pm 4.22					33.12 \pm 1.91
Jul	5128L CL 34.16 \pm 4.89	5129RCLA 24.88 \pm 3.18	5130L CL 32.75 \pm 4.04	5131L CL 34.73 \pm 3.27	5132L CLA 35.78 \pm 3.58						32.46 \pm 4.38
Aug	5137L CL 36.40 \pm 4.33	5138L CL 34.94 \pm 3.79	5139R CL 28.53 \pm 2.51	5140R CL 34.04 \pm 3.67	5141L CL 34.06 \pm 3.79						33.60 \pm 2.99
Oct	5010 CL 30.35 \pm 2.05	5148R CL 36.63 \pm 4.26	5149 CL 29.04 \pm 2.78	5150 CLA 20.66 \pm 2.24	5151 CL 34.83 \pm 3.91	5153 CL 35.52 \pm 3.92					31.17 \pm 5.96
Nov	2958L CL 19.03 \pm 3.08	3014R CL 27.15 \pm 2.82	3024R CL 21.68 \pm 1.77	3032L CL 26.58 \pm 2.92	3033R CL 26.48 \pm 2.82	3134L CL 25.08 \pm 2.54	3143L CL 24.03 \pm 2.11	3144L CL 19.25 \pm 1.88	5154L OCL 27.60 \pm 2.27		24.10 \pm 3.34
Dec	4600R CL 21.78 \pm 1.54	4601R CL 22.91 \pm 1.77	5008R CL 27.00 \pm 2.12	5009L CL 29.03 \pm 2.78	5011R CL 21.24 \pm 1.23						24.39 \pm 3.44
Jan	5012L CA 24.70 \pm 2.58	5156L CA 21.45 \pm 2.20	5157R CA 23.54 \pm 1.72								23.23 \pm 1.65
Mch	AP5R CA 14.13 \pm 2.05	AP6 CAA no cells	AP7R CA 13.02 \pm 1.96	AP8L CA 20.44 \pm 2.33	AP9L CA 18.39 \pm 2.18						16.50 \pm 3.51

NCL = Newly formed CL, CLA / CAA = corpus of abortion

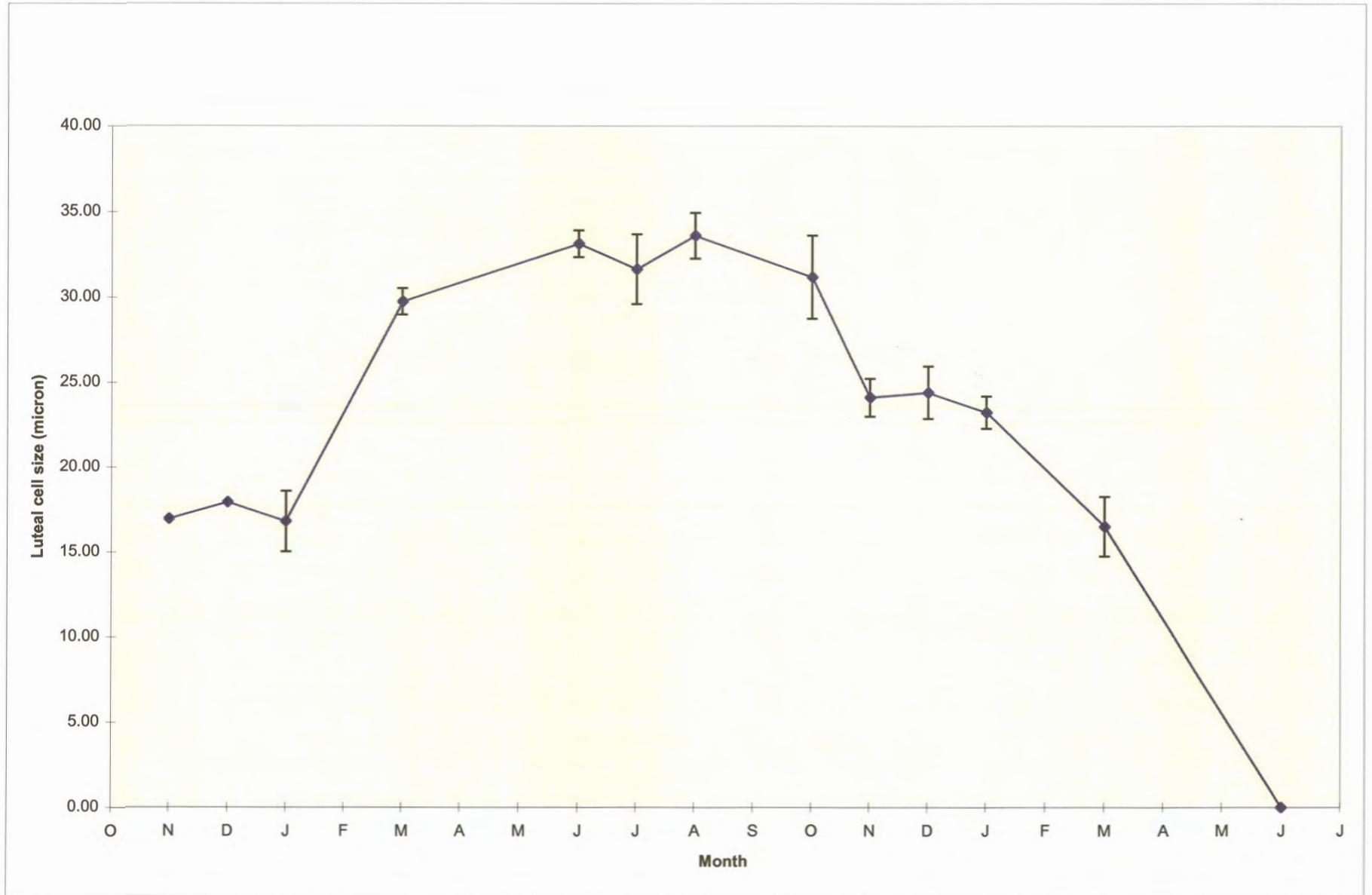


Fig. 9: Average monthly luteal cell sizes (um). Missing months have been interpolated (bars indicate SD, except where sample < 3)

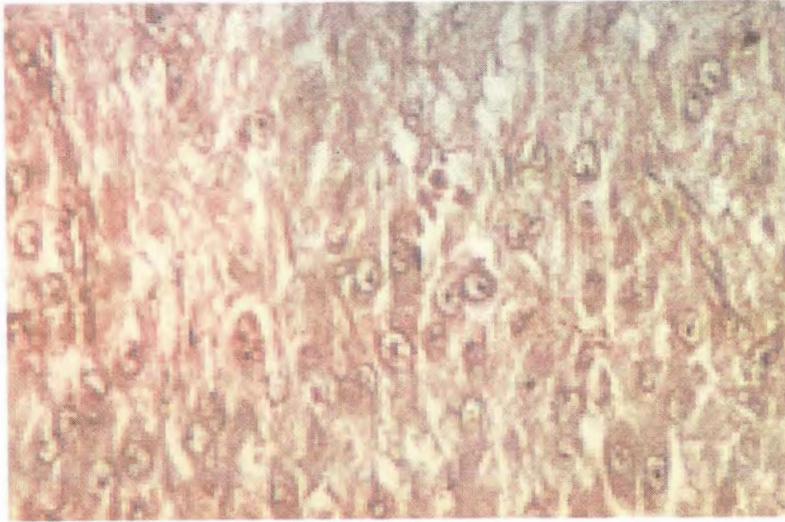


Figure 10: Histological appearance of a young *corpus luteum* in a female of unknown age (4601) in December (400 x)

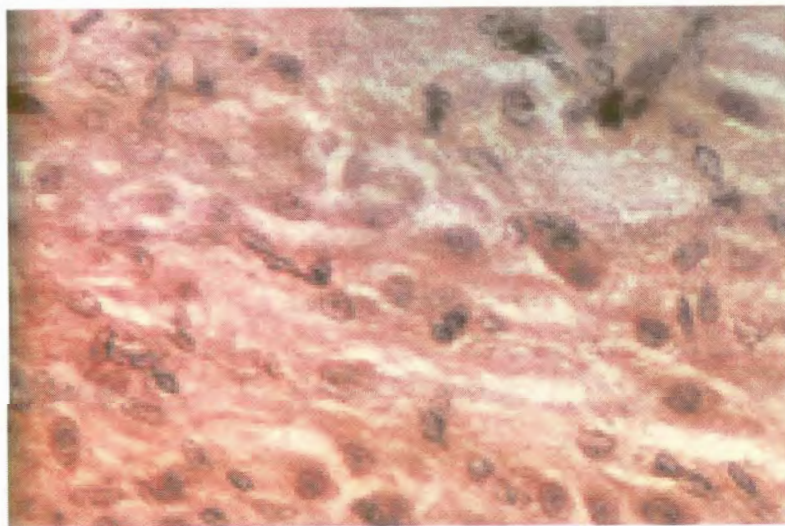


Figure 11: Histological appearance of a young *corpus luteum* in a female of unknown age (5012) in January (400 x)

The CL has increased somewhat in size (average 12.96 ± 1.62 (SD), ranging from 10.87 to 15.40 between individuals), and has still retained the greatly lobulated form. In spite of the thecal folds, the CL has a shape ranging from ovoid to almost spherical (Fig. 12).

By March, the luteal cells have greatly increased in size to about 30 μm . They are somewhat disparate in shape, but all have a roughly round or oval shape with a healthy, central nucleus and prominent nucleolus (Fig. 14). The cytoplasm shows some signs of cellular retrogression, though. It has a smooth, homogeneous appearance in some cells, while some large vacuoles may be present. Large numbers of small vacuoles may occur in the cytoplasm of some cells, though such cells are less common. Large interstitial spaces exist, but the large ovulation cavities have disappeared, luteal cells spreading evenly throughout the body of the CL. The central core has grown smaller, though may still be as much as ≥ 4 mm across and consist entirely of dense connective tissue (Figs. 13).

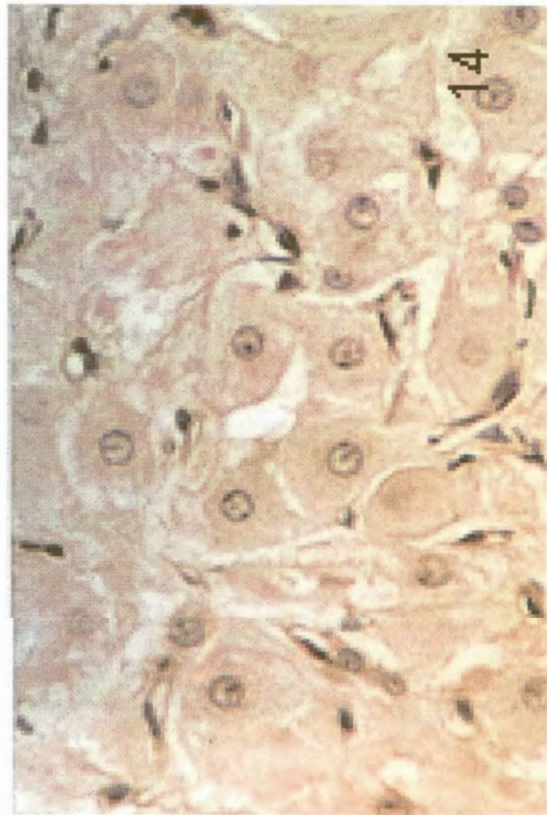
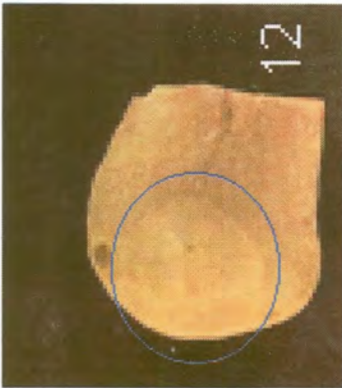
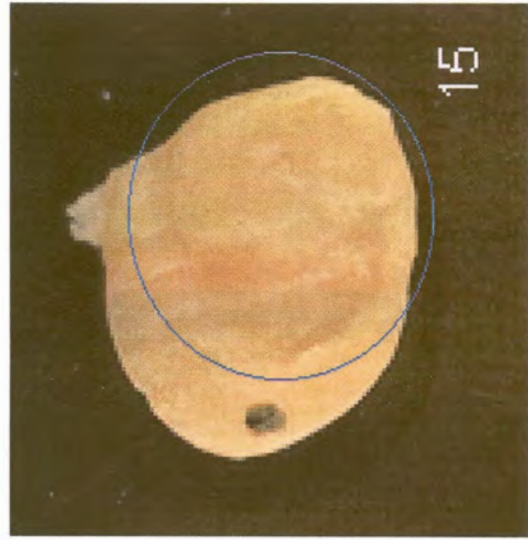
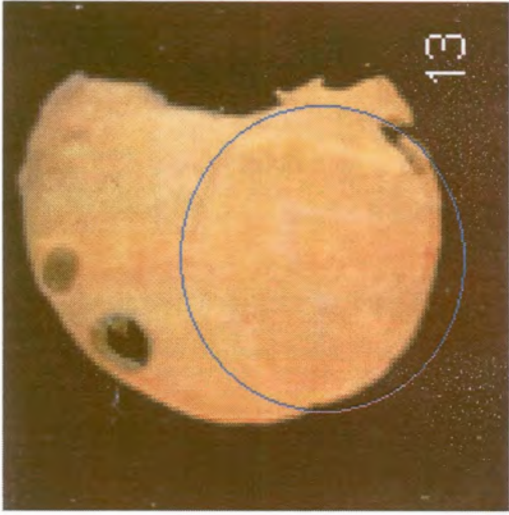
During the same period, the CL has shown only a moderate size increase, (averaging 14.91 ± 1.54 mm), although some variation exists, individual CLs approaching 18 mm (female 946). During April the CL further increases in size (reaching an average of almost 17 mm), filling out and beginning to lose its' lobulated shape (Fig. 15). The core is still visible, though small, decreasing in size even further during May. The thecal folds which have given the CL its lobulated shape have virtually disappeared by this time and the active CL now fills well over half the ovarian volume. No histological material is available for

Figure 12: Macroscopic appearance of a *corpus luteum* in a pregnant (containing an unimplanted blastocyst) 11 year old female (3906) in February

Figure 13: Macroscopic appearance of a *corpus luteum* in a 7 year old female (946) in March

Figure 14: Histological appearance of a *corpus luteum* in a female of unknown age (APP6), in March
(400 x)

Figure 15: Macroscopic appearance of a *corpus luteum* in a pregnant (recently implanted) 5 year old female (3645) in April



this critical implantation (April) and post-implantation (May) period, but there appears to be different rates of luteal growth amongst animals. *Corpora lutea* found in animals in which implantation had occurred in the ipsilateral uterine horn by the time of capture in April ($n = 8$) were significantly larger than CLs in the (unimplanted) animals of March ($t = 4.29$, $df = 25$, $p = 0.00023$), while animals without implanted embryos in April ($n = 7$) did not show such a significant increase from March ($t = 1.36$, $df = 24$, $p = 0.19$). Amongst those animals in the April sample where implantation had not occurred by the time of collection, non-pregnant animals could not be distinguished from pregnant (but still unimplanted) animals.

Luteal growth is continued during June, at which time the CL may occupy as much as 90% of the ovarian volume, averaging about 22 mm in diameter (Fig. 16). The CL has taken on an almost spherical shape, with almost no thecal intrusions being visible in the body of the CL with the naked eye. Microscopically, however, they appear compressed into thin fibrous streaks. The central core, though still visible, has decreased to the smallest size recorded throughout gestation, forming a small dense connective tissue clot of not more than 1 or 2 mm situated at, or close to the centre of the CL (Fig. 18).

Luteal cells have at this stage reached an average diameter of well over 30 μm with the one non-pregnant female (5096) having cells averaging almost 35 μm . Almost all cells are still healthy and active. At this stage, however, some early signs of luteal regression are apparent. The most evident are indications of cell loss, especially close to the central core where large interstitial spaces have

become visible, and luteal cells appear to be replaced, or at least surrounded by loose fibrin. Additionally, but to a lesser extent, interstitial spaces have also increased throughout the body of the CL (Fig. 17). There is also an increase in the level of vacuolization in the luteal cell cytoplasm. One or more very large vacuoles can be seen inside the cytoplasm of a few cells, while smaller, more numerous vacuoles become visible in the peri-nuclear area of some cells under higher magnification. A small number of pyknotic nuclei are also visible. The CL of the one non-pregnant female (5096) in June does not differ noticeably in any way from those of other, pregnant females, and this, together with the presence of a large, raw scar of placentation, suggests a recent termination of pregnancy.

During July, there seems to be a slight drop in the average cell size, although not significantly lower than those of either June ($t = 1.123$, $df = 8$, $p = 0.294$) or August ($t = 0.469$, $df = 7$, $p = 0.653$). Nor is the apparently rather larger drop in the overall size of the CL (Table 4, Fig. 8) significant, compared to June ($t = 1.88$, $df = 17$, $p = 0.08$) or August ($t = 1.50$, $df = 11$, $p = 0.16$). However, a sudden increase in follicular activity, both in follicle numbers (Table 3, Fig. 4) and sizes of the largest follicle (Table 3, Fig. 5) occurred at this time (results, section 3.2).

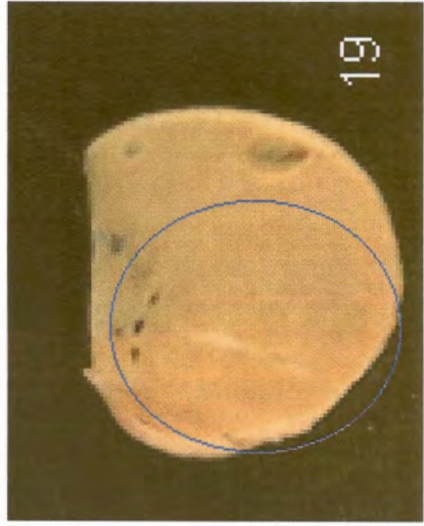
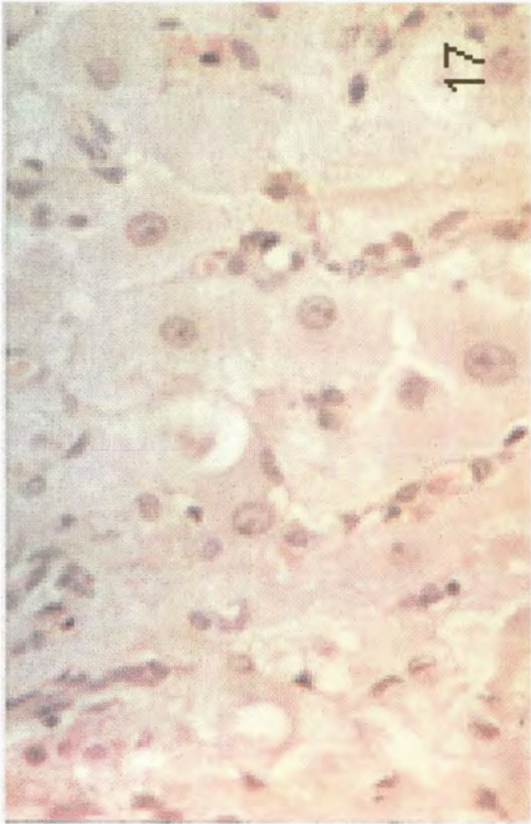
The CL of July has a very similar macroscopic appearance to that of June, with a homogeneous, spherical shape, little apparent thecal penetration into the body of the gland, a distinct periphery with heavy vascularization and a very small core in the centre of the gland (Fig. 19). Most cells have a round or oval, polygonal shape with central, healthy nuclei, prominent nucleoli, and

Figure 16: Macroscopic appearance of a *corpus luteum* in a pregnant female of unknown age (5069) in June

Figure 17: Histological appearance of a *corpus luteum* in a pregnant female of unknown age (5087) in June (400 x)

Figure 18: Histological appearance of the central core of a *corpus luteum* in a pregnant female (5087) of unknown age in June (80 x)

Figure 19: Macroscopic appearance of a *corpus luteum* in a pregnant female of unknown age (5131) in July



homogeneous cytoplasm (Figs. 20, 21 & 22). In general, cells are closely packed, although the early signs of luteal regression observed during June are present, though only slightly further advanced. These include some cellular resorption, as evidenced by the increased interstitial spaces, and a slightly larger connective tissue central core. Further luteal regression is evidenced by the appearance of some fibroblasts, especially in small thecal protrusions into the luteal tissue. Little connective tissue is present inside the body of the CL though, with the exception of those inclusions in the central core and around the periphery of the gland. There is, however, an increase in fibrin which surrounds many luteal cells, being no longer confined to the cells close to the central core. Numerous capillaries also appear inside the luteal tissue, their endothelial cells being visible between luteal cells, while larger capillaries, confined to the luteal core and periphery, have dense connective tissue surrounding them.

During August, the CL reaches its greatest diameter, averaging over 22 mm, with individual corpora exceeding 25 mm. Macroscopically, the CL shows the first signs of losing the homogeneous appearance which had characterized it during June and July. The CL periphery, always prominent and heavily vascularized, now shows a dramatic thickening, with some trabeculae penetrating into the luteal tissue (Fig. 23).

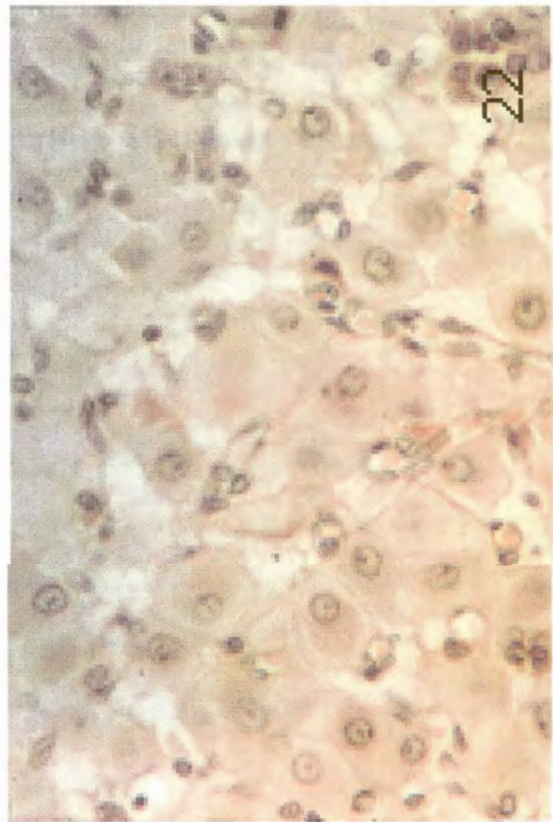
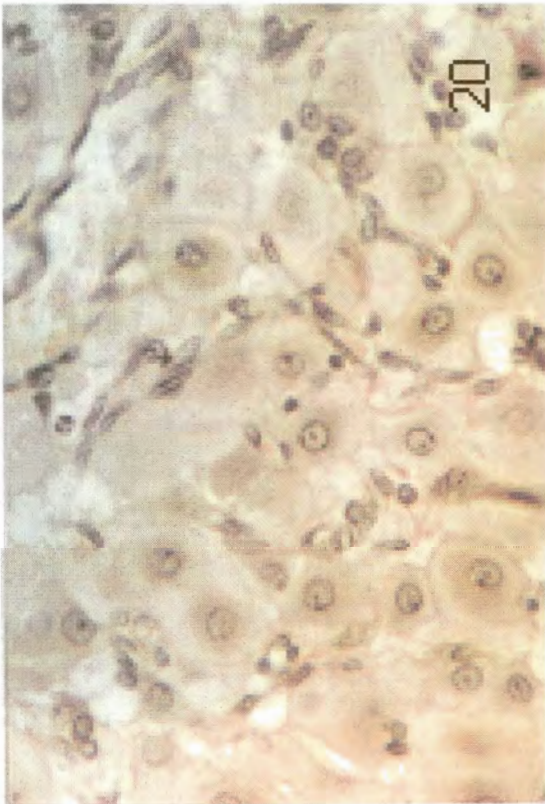
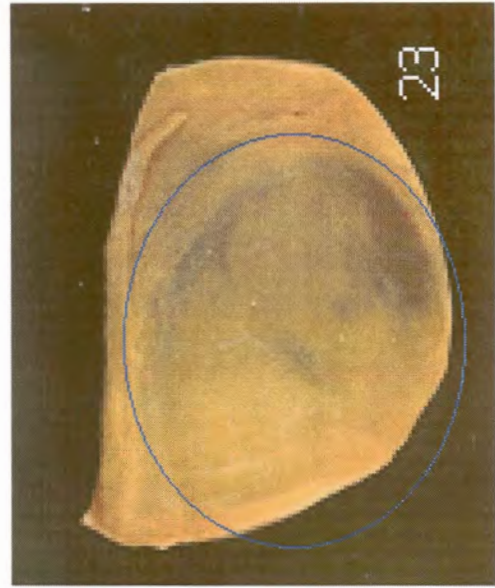
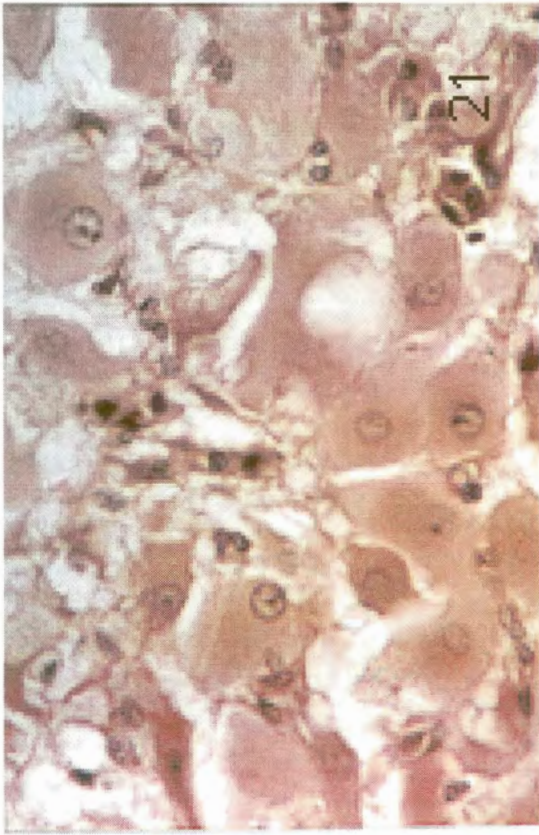
Microscopically, the gland during August has much the same shape as it has had during July, save that the connective tissue component of the gland has increased. Dense connective tissue is noticeable primarily around the central core which had enlarged slightly (though still not more than 3-4 mm), at the

Figure 20: Histological appearance of a *corpus luteum* in a pregnant female of unknown age (5130) in July (400 x)

Figure 21: Histological appearance of a *corpus luteum* in a pregnant female of unknown age (5131) in July (400 x)

Figure 22: Histological appearance of a *corpus luteum* in a pregnant female of unknown age (5130) in July (400 x)

Figure 23: Macroscopic appearance of a *corpus luteum* in a pregnant 13+ year old female in August



periphery of the CL, and inside the invaginating thecal trabeculae which have increased both in number and in size. A fine network of fibrin appears to permeate the corpus, more prominently than during July, interspersing luteal cells throughout the body of the gland, though still most prominently around the core and periphery (Fig. 24). Luteal cells average about 35 μm in size, although there does seem to be some variation between individuals, one female (5139) with a large CL of pregnancy having an average cell size of 28.53 μm . Capillaries are also visible throughout the gland, though still concentrated in certain areas. The larger blood vessels occur deep inside the CL, close to or inside the central core, close to the periphery, or inside the thecal trabeculae, while smaller capillaries are more widespread. Further cell loss is indicated by increased interstitial spaces.

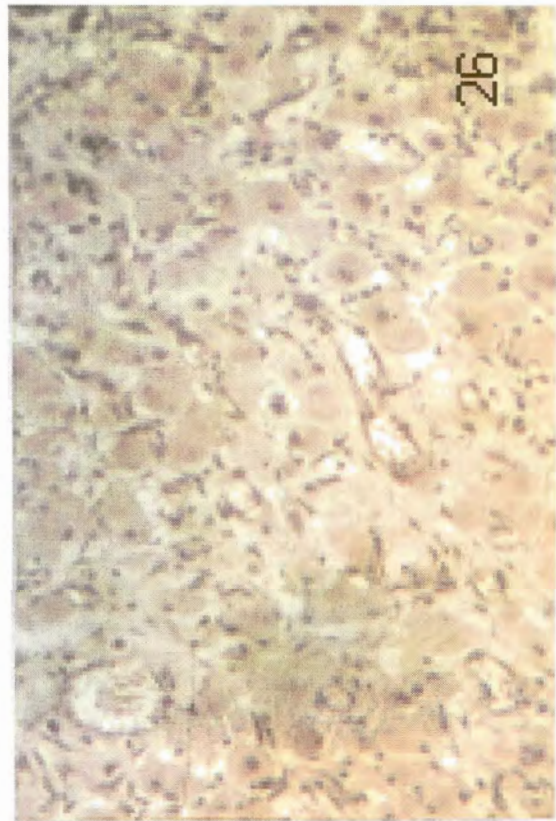
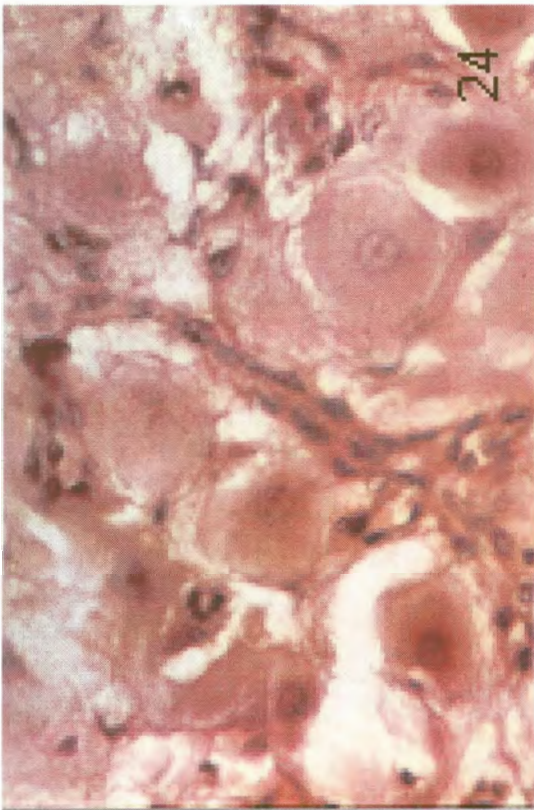
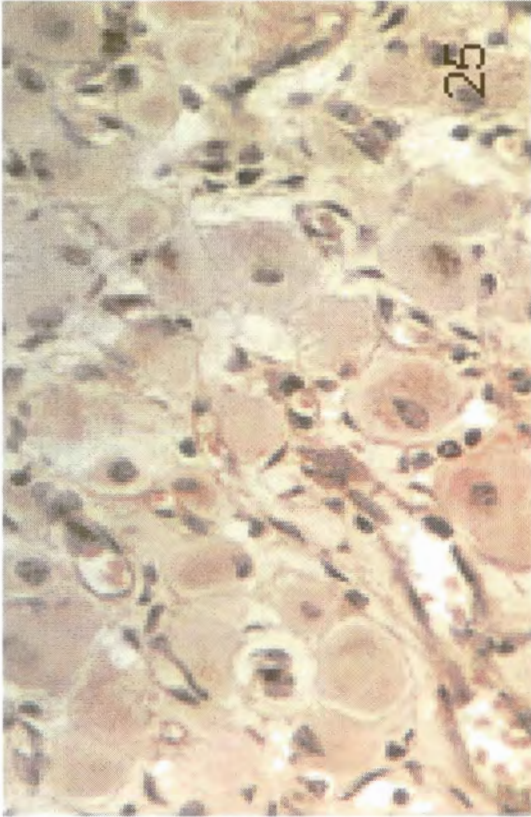
No material is available for September, but during October, definite signs of CL regression are apparent (Figs. 25 & 26). Macroscopically, the central core has greatly increased in size, while connective tissue trabeculae from the CL periphery are very prominent. The CL also shows a reduction in size, falling to < 20 mm in size, although one pregnant female (4093) still had a CL of 26.53 mm in size. The macroscopic signs of regression are coupled to various microscopic signs of luteal regression, such as a reduction in the luteal cell size (Table 5, Fig. 9) though they still average > 30 μm . Very few large vacuoles are visible, but most cells show extensive vacuolization, large numbers of small vacuoles being present throughout their cytoplasm. Many cells also have pyknotic nuclei, and where these occur, they usually lie peripherally in the cellular cytoplasm.

Figure 24: Histological appearance of a *corpus luteum* in a pregnant female of unknown age (5137) in August (400 x)

Figure 25: Histological appearance of a *corpus luteum* of recent parturition in a female of unknown age (5149) in October (400 x)

Figure 26: Histological appearance of the *corpus luteum* of recent parturition in a female of unknown age (5149) in October (200 x)

Figure 27: Macroscopic appearance of a *corpus luteum* of pregnancy in a female of unknown age (3051) in November



Proliferation of fibroblasts is evident, especially in large thecal septae, stretching deep into the luteal tissue, with concomitant increases in dense CT and fibrin in these areas. Extensive capillary beds are present throughout the body of the corpus, larger vessels still being concentrated close to areas of dense connective tissue concentrations, and in the vicinity of the thecal septae.

Female 5149 has a CL with cells averaging $29.04 \mu\text{m}$ and has a very young CH in the ovary contralateral to the ovary with the CL, the horn of which shows evidence of recent pregnancy. The CL of pregnancy is small, but the cells are not in any way obviously different from any of the pregnant females, and it is therefore assumed that the female underwent an early but successful parturition.

The process of luteal regression continues during November. The most evident feature is a further decrease in the cellular size ($24.1 \pm 3.34 \mu\text{m}$), ranging from as small as $19 \mu\text{m}$ in some females, but may still be as large as $27.60 \mu\text{m}$ (in female 5154). Luteal cells show signs of extensive vacuolization, large numbers of small vacuoles being spread throughout the cytoplasm in almost all cells. Luteal cells are still numerous throughout most of the CL (Fig. 28), although large areas are almost devoid of them. These areas may be predominantly acellular (with fibroblasts constituting the cellular component) and occur primarily close to the periphery or the centre of the CL, or they may be largely cellular (with some dense and loose CT interspersed), with the cellular component comprising fibroblasts, macrophages and capillary endothelial cells, and occur anywhere within the gland. Thecal trabeculae have extended further into the CL (Fig. 27). These trabeculae have lost most of their cellular

components, consisting primarily of dense connective tissue strands reaching towards the central core. The central core has likewise increased in size, forming a large, stellate core of dense connective tissue with strands of connective tissue radiating towards the glandular periphery. These connective tissue strands may merge, connecting the core with the periphery.

During December, the CL averages 16.14 ± 2.12 mm. The luteal cells have also hypotrophied, averaging 22.55 ± 1.78 μm . Luteal cells are still numerous, although there is a proliferation of non-luteal cellular components, each luteal cell being surrounded by one or more layers of fibroblasts - laying down connective tissue between luteal cells - or capillaries. Although there are still luteal cells with a healthy appearance, most have a ragged, irregular shape. Most are resorbing, leaving a clear margin surrounding them, indicating the level of cellular hypotrophy. Nuclei may lie either centrally or peripherally in the cell, but most are pyknotic. The cytoplasm has taken on a very smooth, homogeneous appearance, and no vacuolization is apparent. Luteal activity has probably ceased at this stage. Capillaries are widespread throughout the glandular body, each with a thick layer of connective tissue surrounding it. In some areas, these capillaries occur in groups, forming small, stellate-shaped connective tissue areas filled with blood vessels similar in appearance to the central core, though smaller and occurring anywhere within the CL.

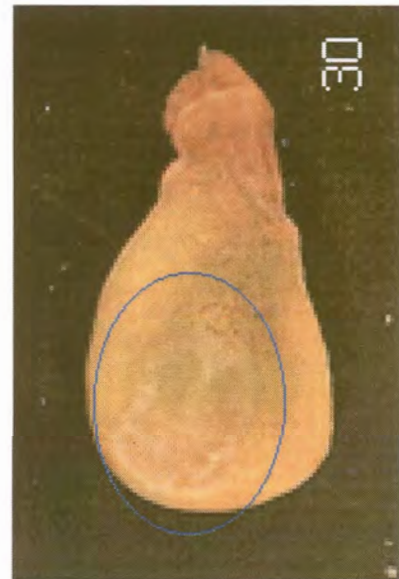
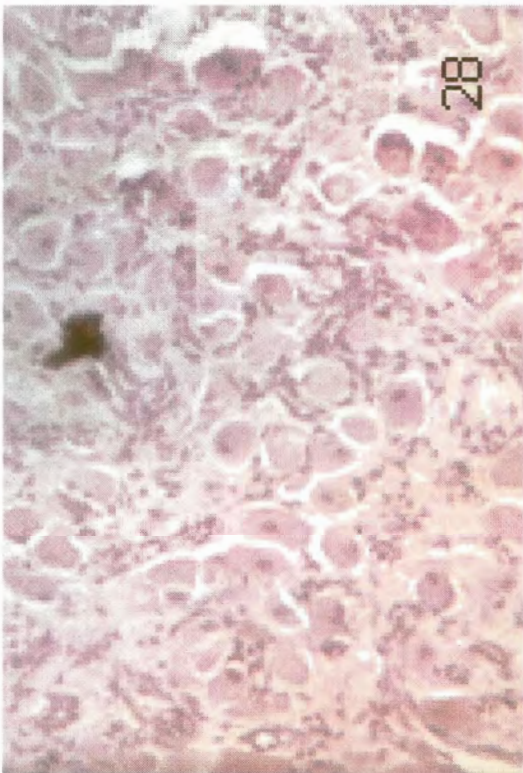
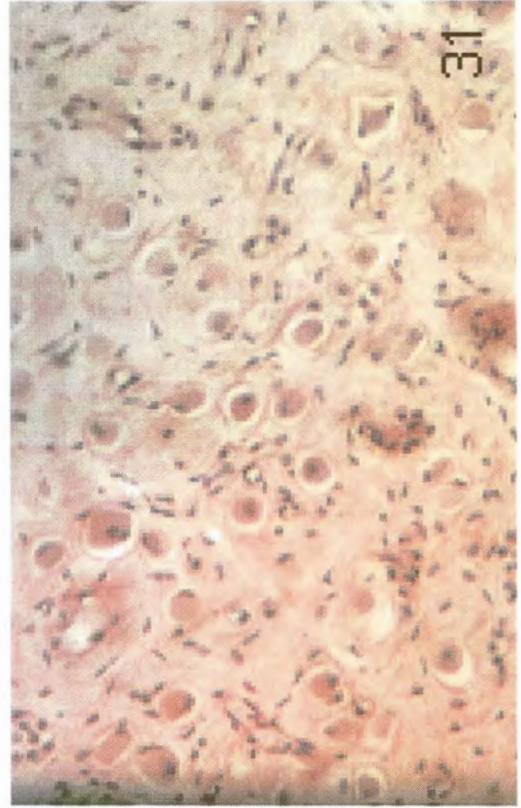
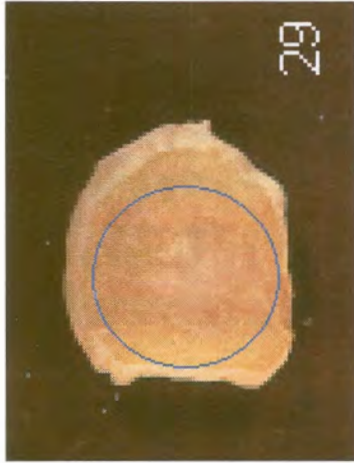
The post-partum luteal regression (from January onwards) appears to be gradual. Figs. 29 and 30 show relatively amorphous structures in January and

Figure 28: Histological appearance of a post-partum *corpus luteum* in a female of unknown age (5154) in November (200 x)

Figure 29: Macroscopic appearance of a *corpus albicans* of previous pregnancy in an 8 year old female (3803) in January

Figure 30: Macroscopic appearance of a *corpus albicans* of previous pregnancy in a 10 year old female (3898) in February

Figure 31: Histological appearance of a *corpus albicans* of previous pregnancy in a female of unknown age (APP9) in March (200 x)



February respectively in which the CL periphery is merging with the surrounding ovarian stroma. The central core and periphery of connective tissue appear to have disappeared as separately discernible entities, having merged to form a seemingly almost homogenous mixture of cellular and connective tissue components. Ovarian stromal cells have begun penetrating the body of the CL.

In March, luteal cells are still present, though very small ($16.8 \pm 3.99 \mu\text{m}$). Many luteal cells are anuclear, the remainder have pyknotic nuclei. Additionally, the cytoplasm appears very smooth, yet cells may still be numerous and large at this stage (e.g. female 5157).

The appearance of luteal cells during March is shown in Figs. 31 and 32. Luteal cells are clearly demarcated and round, almost spherical, although some have a ragged, smaller and less regular shape. Variation occurs between individuals, but cellular sizes average $16.5 \pm 3.51 \mu\text{m}$. Cellular constituents of the CA are predominated by fibroblasts, laying down connective tissue which is at this stage the dominant component of the CA. Vascularization is still extensive in the periphery while an extensive capillary network exists throughout the CA. Nuclei are either absent or pyknotic.

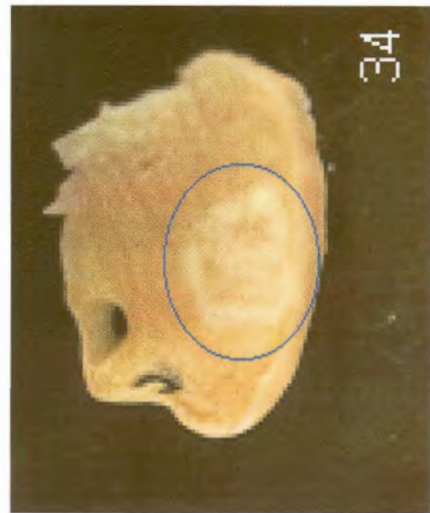
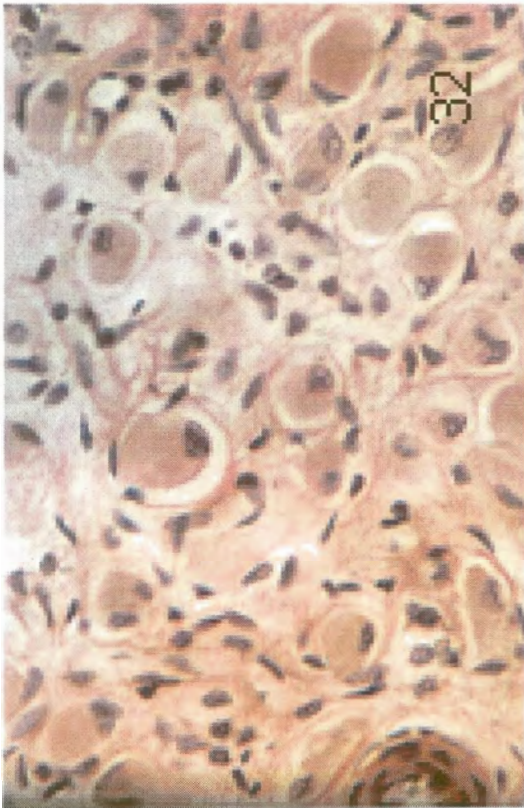
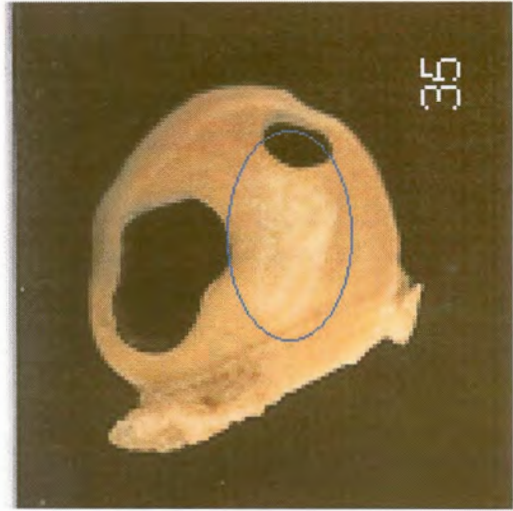
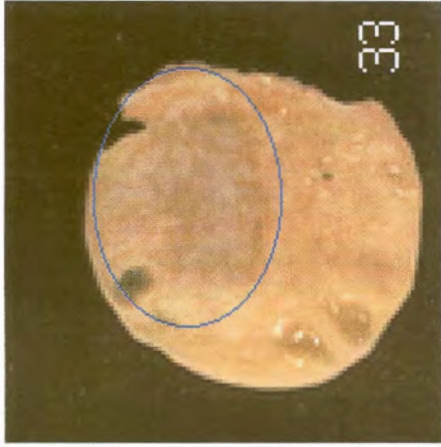
Histological information is absent for April and May, but CA resorption appears to continue slowly and gradually after March, around the time of implantation in the contralateral uterine horn (Figs. 33 & 34) and by June, no luteal cells are visible. The general appearance of the *corpus albicans* at this stage is of a central, stellate-shaped core of dense connective tissue in the centre of the structure, a thick ring of dense connective tissue around the

Figure 32: Histological appearance of a *corpus albicans* of previous pregnancy in a female of unknown age (APP6) in March (400 x)

Figure 33: Macroscopic appearance of a *corpus albicans* of previous pregnancy in a 5 year old female (3645) in April

Figure 34: Macroscopic appearance of a *corpus albicans* of previous pregnancy in a 13+ year old female (3238) in May

Figure 35: Macroscopic appearance of a *corpus albicans* of previous pregnancy in a female of unknown age (5039) in June



periphery, merging with the ovarian stroma, and the remainder being filled with fibrin, fibroblasts, macrophages and blood capillaries (Fig. 35).

Due to a lack of relevant histological material, it can not be said with any certainty when luteal cells finally disappear, though it can be either during April or May (i.e. during, or shortly after the presumed reactivation of the CL in the opposite ovary, followed by implantation in the uterine horn ipsilateral to the ovary with the newly activated CL). Further regression of the CA after June appears to be limited to a reduction in the size and the cellular components of the CA (Fig. 36). Vascularization is reduced accordingly, and by August, the corpus consists of an amorphous, virtually acellular structure of dense connective tissue (Figs. 37 & 38), rapidly shrinking and merging with the ovarian stromal tissue, consolidating around the central core.

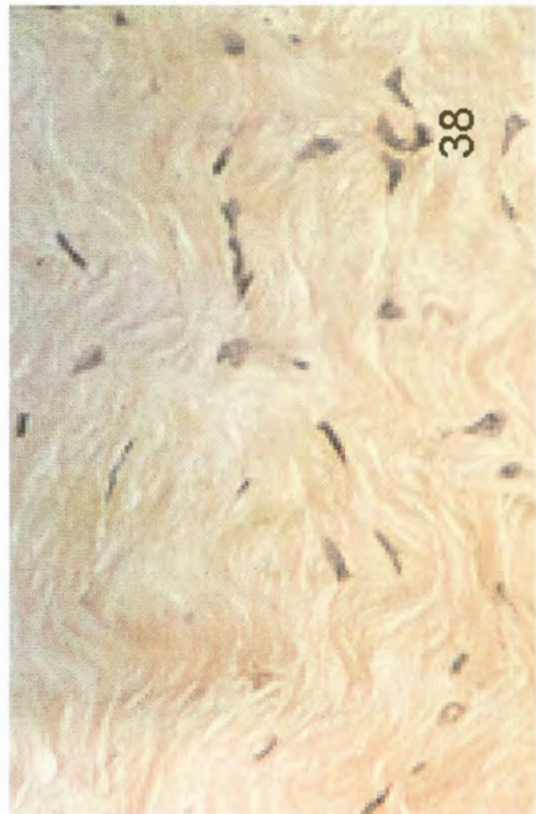
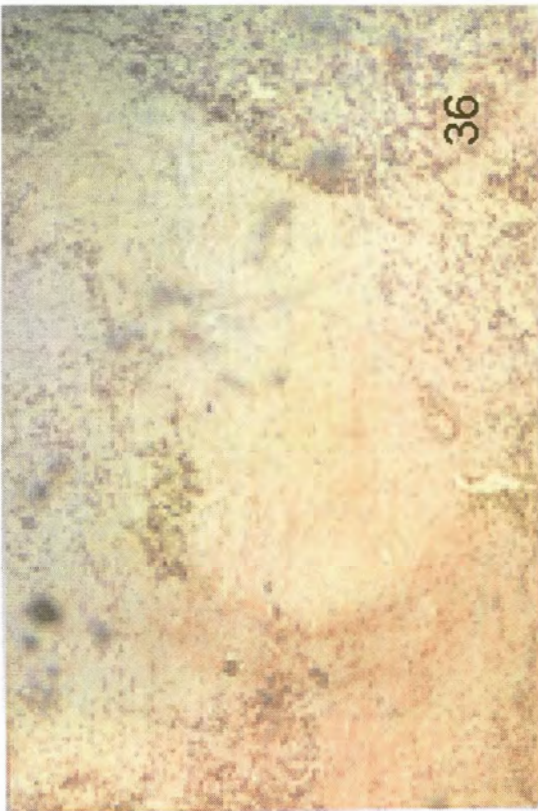
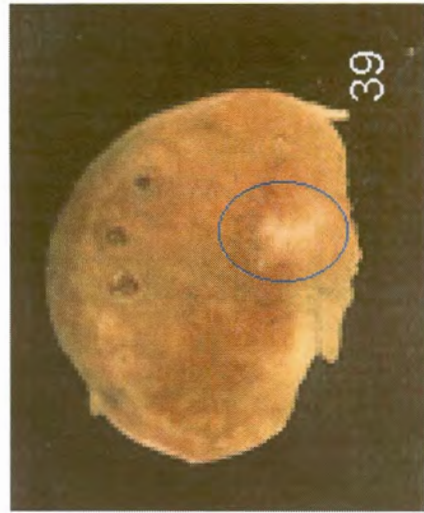
By the following December, all that remains of the two year old CA is a small white scar which may have strands of dense connective tissue radiating outwards from it (Fig. 39). This structure may occur anywhere in the ovary which is itself about to, or has already ovulated once more. At this stage, the old CA may exist together with the newly formed CL. With the final disappearance of the luteal cells during, or before June of the second year following the formation of the *corpus luteum*, the synchronization in the luteal cycle which had persisted until then seems to break down, and there appears to be great variation in the rate at which the CA regresses to the point at which it is no longer identifiable. Two CAs observed during December were still large (9.78 and 8.40 mm respectively), and were merely white scars in the body of the ovary (Fig. 39),

Figure 36: Histological appearance of a *corpus albicans* of previous pregnancy in a female of unknown age (5132) in July (80 x)

Figure 37: Histological appearance of a *corpus albicans* of previous pregnancy in a female of unknown age (5139) in August (80 x)

Figure 38: Close up of dense connective tissue of the type shown in Figures 36 and 37 (400 x)

Figure 39: Macroscopic appearance of a *corpus albicans* of previous pregnancy, two years after formation, in a female of unknown age (5008) in December



although a third was much smaller, and could only be confidently distinguished from a *corpus atreticum* by histological examination.

After December, as the CA enters its third year, it can still be very large, and may remain easily identifiable into its fourth year but great variation in the rates of resorption between animals exists at this stage. Commonly, the CA is at this stage easy to confuse with a *corpus atreticum*, and positive macroscopic identification of the CA can be done with decreasing confidence between about November or December of its second year (when placental scarring is still visible as an aid as described in the following section) and August of its third year. Any identification of CAs after this can be said to involve a fair amount of guesswork, although it seems as though the CA may still remain in the ovary long after this, though often only visible under a microscope.

An interesting feature of CAs during these final stages of resorption is that, while variation in the sizes of 3rd CAs are large, ranging between < 2 mm (eg. female 5096 in June) to around 7 mm (e.g. female 4413 in March or female 4070 in August), 3rd CAs did not differ significantly from 4th CAs in size in the 11 cases where both of these were identified in the same female ($t = 0.85$, $df = 20$, $p = 0.404$). This may be ascribed to either highly variable rates in CL resorption, or to double ovulations, though which option is correct in each case can not be determined with any confidence. Furthermore, in appendix 1 it can be seen that the 4th CA is often larger than the 3rd CA. This may be indicative of a breakdown in the strict alternation of ovulation between ovaries which had otherwise been observed, although this can only be speculated upon.

The cycles of CL and luteal cell growth are shown graphically in Figs. 8 & 9, from the time of formation until such time as the luteal cells disappear, or the *corpora albicantia* cease to be readily identifiable. A significant correlation exists between the size of the CL/CA and the size of the luteal cells ($R = 0.70$, $F = 53.20$, $df = 1,155$, $p = 0.000001$) (Fig. 40).

3.4) Pregnancy, placental scarring, delayed implantation and gestation

The presence/absence of placental scarring is listed in appendix 1. Little qualitative information is available, due to the variable nature of the available material. Three small CAs are present in the December sample. Two of these females (4600 & 5008), with large CAs, have readily visible areas of placental scarring which show up as light orange against the pale, very light brown (almost white) background of the mucosal tissue. The third CA, 1.64 mm in size (female 5011) was not accompanied by evidence of scarring in the ipsilateral uterine horn and the CA has therefore either resulted from a non-pregnant cycle, or a failed reproductive cycle caused either by a failure to implant, or an abortion shortly afterwards. Placental scars are still clearly visible during October in females with large *corpora albicantia*, but invisible in females with failed pregnancies. It is therefore assumed that placental scars remain easily visible for at least a year post-partum in females with successful reproductive cycles.

Females with missed or failed pregnancies apparently show no scarring by the second half of the year following the start of the new reproductive cycle.

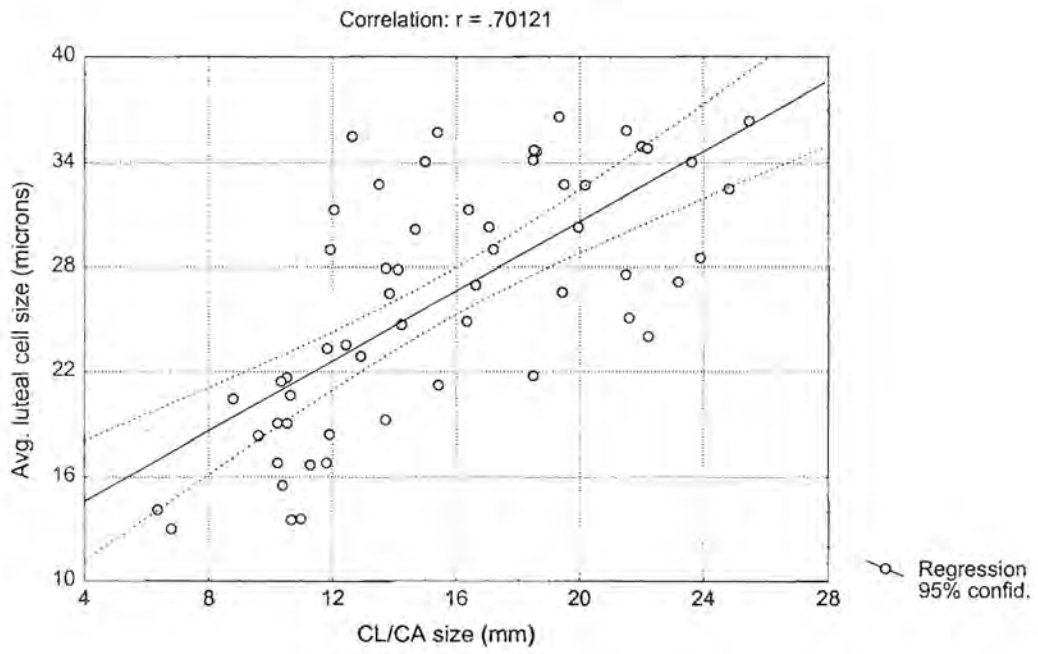


Fig. 40: Regression analysis of luteal cell sizes (μm) vs. CL / CA size

Little evidence of pregnancy was found during the post-ovulatory/pre-implantation period, save for a single unimplanted blastocyst observed in an 11 year old female in February and a further three observed in March in two 14 year old females and one 10 year old. During April, the first 8 females (out of $n = 17$) with implanted embryos were observed. One of these (female 3975) was a 4 year old female in its first reproductive cycle, the remaining seven females ranged from 5-11 years and had all been pregnant during the previous reproductive cycle (all had large resorbing CAs in the non-pregnant ovary), while all but one (female 3645) had large zonary bands in the uterine horn ipsilateral to the ovaries with the CAs.

Five females had not implanted by the time of collection (10-15 April), all of which had undergone at least one previous reproductive cycle, although three of them had probably undergone premature terminations of pregnancy during the previous year (no uterine scarring was apparent, and all had very small, highly resorbed CAs). Two animals in the April sample were obviously pre-pubertal, as evidenced by the lack of any *corpora lutea/albicantia*, or mature follicles, and they therefore showed no signs of incipient or previous pregnancy.

As described in the previous section, the average size of the CL in animals with implanted embryos was significantly larger than CL size in March. The average CL size in animals without implanted embryos, on the other hand, was not significantly larger than that of March, providing circumstantial evidence for a possible pre-implantation reactivation of the CL at this time in some females. By May, implantation appears to have been concluded as eight animals

with CLs had implanted embryos. A further three animals were sexually immature, while a fourth (an 8 year old female, 3293) did not possess either an implanted embryo, or a CL. A large CA from the previous reproductive cycle in one ovary, with a large ZB in the uterine horn ipsilateral to that ovary, however, showed that this animal was sexually mature. This was the only observed failure to ovulate by a sexually mature animal in this study. This sample does not allow for a precise estimation of the time of implantation. However, no animals had implanted by the end of March, but by 15 April, 8 out of 15 animals with CLs (53.3% of the April sample) had implanted, which then implies that the median date of implantation occurs before the middle of April.

With the exception of two 3 year old pre-pubertal animals (females 4064 and 4154), all other animals in the June, July, August and October samples ($n = 46$) had ovulated, and, except for a 3 year old first-time ovulator (4129), all had both mated and implanted successfully. A number of these had, however, undergone subsequent premature terminations of pregnancy, as indicated by the presence in each of a large CL in one ovary, a large, raw, orange ZB in the uterine horn ipsilateral to the ovary with the CL, and the absence of a foetus in that same uterine horn (females 5096 (June), 5129 and 5132 (July), 4070 (August) and 5150 (October)).

October sees the beginning of the breeding season, and the first ovulations ($n = 5$) were observed. Out of 14 sexually mature animals, 11 were either pregnant, ($n = 6$) or showed signs of having recently given birth (i.e. healthy CLs and large, raw scars of placentation ($n = 5$)). Only one of these had

an interrupted pregnancy (5150), signs of foetal resorption having been recorded upon collection in the uterine horn ipsilateral to a small, resorbing CL with small, regressing cells. The remaining four (4131, 5010, 5149 & 5153) are all assumed to have undergone pregnancy to term, due to the inability of distinguishing late-pregnancy abortions/resorptions from early full-term parturitions, without directly observing pupping or abortion. The other three October females (4111, 4136, 4147) are all assumed to have had failed reproductive cycles, due to the presence of a small, regressive CL in each, and in two cases where zony bands were observed, these were exceptionally small and faint.

No uterine samples were available for November, and reproductive history had to be deduced from the appearance of the CL alone. Four females were found with very small CLs, regressed to the point of not having luteal cells, each corpus consisting of some connective tissue, merging with the ovarian stroma. This suggests that ovulation had taken place, but that the reproductive cycle must have been interrupted some time later.

The remaining 26 females show much variation, both in CL size, and the sizes of luteal cells, but none of them can be said with any confidence to have undergone failed pregnancies. An exact estimation of the date of parturition, which can only be done with certainty with direct observation of an animal, was impossible. Five sexually mature animals out of a total of 15 (33.3%) had ovulated by the end of October. New ovulations were scarce in the November sample (only 3 out of 30 had ovulated), but by December, 3 animals out of five (66.6 %) had ovulated. A fourth (female 5008) had recently given birth (as

indicated by a large CL of pregnancy, with large luteal cells, 27 μm in diameter, with a large ZB), and was probably collected during the week long post-partum, pre-ovulatory period. All animals in the January sample had new CLs, indicating the breeding season to last from October up to the middle of January, when the last females had been collected.

3.5) Pregnancy rates

Table 6 shows the pregnancy rates as calculated for all post-implantation (May to December), post-pubertal animals. Out of a total of 92 post-pubertal animals, 83 were found to be pregnant. This included animals with implanted embryos, with foetuses, or with signs of having implanted, based on evidence of CAs and placental scarring. The remaining nine were non-pregnant. These included two animals in May in which implantation had possibly failed to occur, or were not pregnant. One female (3293) had not ovulated, the only certain failure to ovulate by a sexually mature female in this study. Two females in October were non-pregnant, and showed no signs of having implanted blastocysts. Because of the lack of uterine material in November, it is unknown whether or not the four females deemed to have been non-pregnant had implanted or not. The highly resorbed state of their CLs, based on CL size, cell size (or cell presence) and general CL appearance made it unlikely that implantation had in fact taken place. According to this, 90.2% of females were pregnant, while 9.8 % of post-pubertal females were non-pregnant, or had a blastocyst which failed to implant. This

Table 6: Pregnancy rates for the current reproductive cycle (based on presence of CLs and foetuses/placental scars) and birth rates for the previous reproductive cycle (based on the presence of CAs and placental scarring).

Month	Pregnancy rates		Birth rates	
	Pregnant	Non-pregnant	Implanted	Presumed abortion
Jan	-	-	17	1
Feb	-	-	5	1
Mch	-	-	14	5
Apr	-	-	11	3
May	8	3	6	2
Jun	15	0	7	1
Jul	7	0	5	1
Aug	9	0	9	-
Sep	-	-	-	-
Oct	13	2	11	1
Nov	26	4	-	-
Dec	5	-	2	1
Total	83	9	87	16
% of Total	90.2 %	9.8 %	84.5 %	15.5 %

Table. 7: Age specific pregnancy rates, estimated from presence of embryos, fetuses, active *corpora lutea* and recent placental scarring

Age (years)	Number of age x	Number pregnant in age x	% Pregnant of age x
3	6	1	16.6
4	7	5	71.4
5	6	3	50.0
6	11	10	90.9
7	10	6	60.0
8	8	5	62.5
9-12	12	10	83.3
13+	23	20	87.0

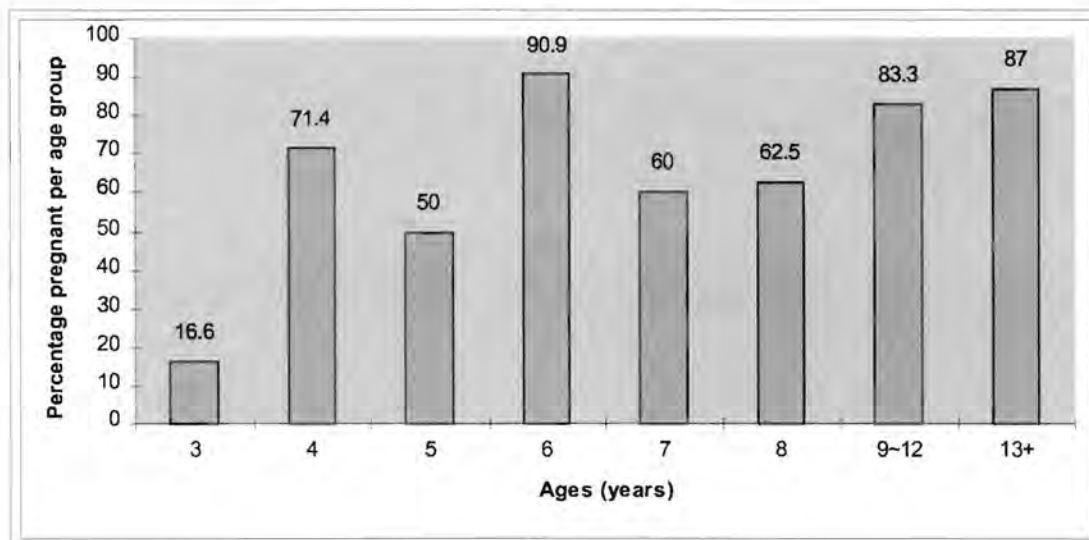


Fig. 41: Age specific reproductive rates, estimated from the presence of embryos/fetuses, active *corpora lutea* and recent placental scarring

can be compared to the birth rates for the previous reproductive cycle (Table 6), determined on the basis of placental scarring and the presence, size and general appearance of CAs. Excluding animals without reproductive cycles during the previous year (animals which were primiparous or pre-pubertal when killed), and excluding the entire November sample (due to the variable nature of CA resorption at that stage - as described in the section on luteal regression, and the lack of uterine material from which placental scarring could otherwise have been determined), 103 animals were used in this calculation. Of these, 87 females (84.5%) showed signs of pregnancy, while 16 females (15.5%) had ovulated, but without apparently becoming pregnant.

Table 7 shows the age specific pregnancy rates, with age class 9-12 years lumped due to small sample sizes. Age-specific pregnancy rates showed an erratic pattern between age classes, but certain trends can be observed in Table 7 and Fig. 41. These include an initial low pregnancy rate (in the 3 year old group), followed by a rapid increase thereafter with pregnancy rates peaking at 6 years. Pregnancy rates fluctuated after this, but showed no obvious decrease in the older (13+) age group.

4.6) Age at puberty & age at sexual maturity

Table 8 shows the age at puberty, back calculated to the previous year, based on the ages and the reproductive history of animals during the previous reproductive

cycle. The average age at puberty, or the average age at which animals first start ovulating is estimated at 4.44 years ($n = 51$ females). Table 9 shows a second estimate of the average age at puberty, where the ages and reproductive history for the previous reproductive cycle are used, except where 2nd CA have been identified, in which case the reproductive history for those animals from two years back are used. In this case, the average age at puberty is calculated as 4.41 years ($n = 52$ females). Table 10 shows the calculations for the age at sexual maturity, the age at which animals can first become pregnant (and implant a blastocyst). Because the origin of CAs could not be ascertained for 2nd CAs, only 1st CAs were used in back calculating to age of sexual maturity, which was estimated to be 5.21 years.

4.7) Prenatal mortality

Table 11 and Fig. 42 show a comparison between CLs/CAs of pregnancy and CLs/CAs resulting from missed pregnancies, as well as from abortions. No apparent differences between *corpora lutea* in pregnant and in non-pregnant animals were observed in the pre-implantation period, and material collected between January and April are shown together. After April, differences between the *corpora lutea* of pregnancy and non-pregnancy / abortion seem to become apparent, CLs of pregnancy (i.e. May to December) being significantly larger than CLs of abortion ($t = 6.534$, $df = 91$, $p = 0.000001$) and CAs (after December) from successful reproductive cycles being significantly larger than those resulting from non-pregnant

Table 8: Average age at puberty, back calculated using 1st CA

Age (years)	n observed	n ovulated	f(x)	P(x)	(x)P(x)
2	2	0	0	0	0
3	11	3	0.27	0.27	0.81
4	7	5	0.71	0.44	1.76
5	10	9	0.90	0.19	0.95
6	10	9	0.90	0	0
7	9	8	0.89	-0.01	-0.07
8	2	2	1.00	0.11	0.89
$\Sigma(x)P(x)$					4.34 years

Table 9: Average age at puberty, back calculated using 2nd CA where available

Age (years)	n observed	n ovulated	F(x)	P(x)	(x)P(x)
2	2	0	0	0	0
3	11	3	0.27	0.27	0.81
4	8	6	0.75	0.48	1.92
5	13	12	0.92	0.17	0.85
6	8	7	0.875	-0.05	-0.30
7	9	8	0.89	0.02	0.14
8	1	1	1.00	0.11	0.89
$\Sigma(x)P(x)$					4.31 years

Table 10: Average age at sexual maturity, using only placental scarring and 1st CA

Age (years)	n observed	n implanted	f(x)	P(x)	(x)P(x)
2	2	0	0	0	0
3	11	3	0.27	0.27	0.81
4	7	3	0.43	0.16	0.64
5	10	8	0.80	0.37	1.85
6	10	7	0.70	-0.10	-0.60
7	9	7	0.78	0.08	0.56
8	2	2	1.00	0.22	1.76
$\Sigma(x)P(x)$					5.02 years

Table 11: Sizes (mm) \pm SD of *corpora lutea/albicantia* of successful pregnancy and of abortion (PM = prenatal mortality, referring both to missed pregnancies and abortions)

	CL/CA of pregnancy	CL/CA of PM
January	12.28 \pm 1.66 (n=20)	
February	12.96 \pm 1.62 (n=6)	
March	14.91 \pm 1.54 (n=19)	
April	16.78 \pm 1.79 (n=15)	
May	17.50 \pm 2.17 (n=10)	15.69 (n=2)
June	21.97 \pm 2.42 (n=14)	18.60 (n=1)
July	18.88 \pm 4.83 (n=5)	15.87 (n=2)
August	22.28 \pm 3.38 (n=8)	8.53 (n=1)
September		
October	19.46 \pm 4.97 (n=10)	9.25 \pm 1.39 (n=5)
November	18.97 \pm 4.10 (n=26)	8.39 \pm 1.06 (n=4)
December	16.14 \pm 2.12 (n=5)	none
January	13.00 \pm 1.47 (n=16)	6.23 (n=2)
February	13.15 \pm 2.36 (n=5)	3.72 (n=1)
March	10.29 \pm 2.25 (n=13)	7.07 \pm 1.81 (n=6)
April	12.26 \pm 2.12 (n=11)	8.13 (n=3)
May	11.56 \pm 1.82 (n=6)	6.37 (n=2)
June	9.75 \pm 1.06 (n=6)	3.99 (n=2)
July	10.47 \pm 0.88 (n=5)	8.23 (n=1)
August	8.78 \pm 1.84 (n=9)	none
September	none	none
October	8.51 \pm 1.80 (n=10)	3.33 (n=2)
November	4.86 \pm 2.46 (n=24)	
December	6.61 \pm 4.35 (n=3)	

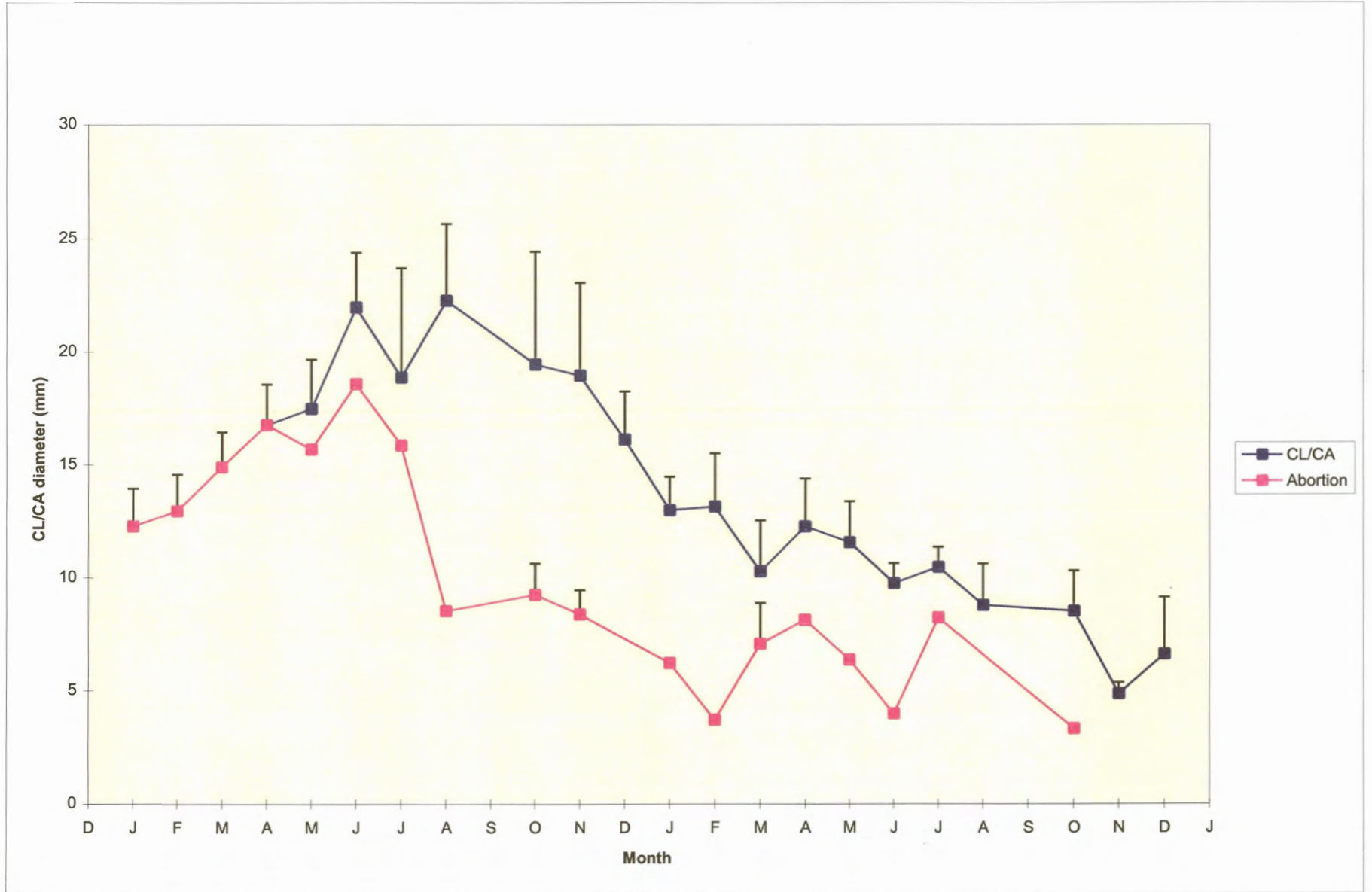


Fig. 42: Comparison between sizes of CLs/CAs of abortion/missed pregnancy, and of CLs/CAs of pregnancy respectively. Missing error bars indicate sample size <3.

or aborted cycles ($t = 7.923$, $df = 98$, $p = 0.000001$). The differences appeared to be very slight at first.

All pre-natal mortalities available for June and July are recent post-implantation abortions. Of the three females (5096, 5129, 5132), macroscopic appearances are identical to *corpora lutea* of pregnancy, and it is only with histological techniques that some differences can be observed in one of the females (5129). She has luteal cells substantially smaller than those of the pregnant females in July, but few other indications of luteal regression are apparent, save for a slightly advanced state of vacuolization and cell loss, though not dramatically different from those of pregnant females in July.

The first highly resorbed CL was only observed during August (female 4070 - 13+ yrs). The corpus is in an extreme state of resorption, and has lost the general CL appearance, being a round, darkish structure without clear border, seemingly merging with the surrounding stroma. No clear histological sections could be made of the ovaries of this female, but this *corpus luteum* was similar in appearance to those of the four females in November, deemed to have had missed pregnancies (females 2929, 2956, 2957 & 3126 - appendix 1). These CLs had no luteal cells, and had the general appearance of an area within the ovary consisting of dense connective tissue and stromal tissue, similar in appearance to the CAs of pregnancy in June or July (i.e. at least six month post-partum), though with less connective tissue and more stromal invasion and a periphery not as readily identifiable. The CLs appeared not to consolidate around a small central scar of dense connective tissue, as is the fate of CLs of pregnancy, but rather to keep their shape and

gradually shrink and fade into the surrounding stroma. This was the general appearance of the single abortion observed also in March (female APP6). Other CLs of abortion showed the general pattern of luteal regression, though only with states of resorption several months advanced, as compared to CLs of pregnancy.

The samples of available abortions are very small (as shown in Table 11). Possibly as a result of this, along with the fact that all abortions are shown together in Table 11 and Fig. 41, irrespective of whether it had been formed from a missed or a failed pregnancy, the sizes of *corpora lutea/albicantia* of abortion are very erratic. There is an indication, however, that following an initial sharp drop in CL size towards August, CL/CA resorption is subsequently retarded. CAs of pregnancy and of prenatal mortality then approach each other in size. The natural variation in the sizes of CLs/CAs between females result in the presence of large corpora of abortion or small corpora of pregnancy which may be confused. Placental scarring aided in determining origins of CLs/CAs between one and two years post-partum. Even so, the 15.5% incidence of prenatal mortality shown in Table 6 may have been slightly underestimated.

No way to circumvent such uncertainty can be suggested, save with direct observation in the field of either parturition or abortion.

Chapter 4: Discussion

A period of delayed implantation is a common feature in many marsupial and eutherian mammals, facultative in many, but common and obligate in particularly the mustelids, ursids, otariids and phocids (Renfree & Calaby 1981, Riedman 1990). In the pinnipeds, this character may be a rule rather than an exception, Boshier (1981) reporting its presence in all six genera of otariids and nine of ten genera of phocids, apparently absent only in the genus *Hydrurga* (Harrison & Kooyman 1968) while Harrison (1969) strongly doubted its existence in the walrus *Odobenus*. Siniff & Stone (1985), however, report it to exist even in the leopard seal (*H. leptonyx*), a period of delayed implantation ranging between early January and mid-February, or about 48 days, while Fay (1981b) reports its presence in the walrus *O. rosmarus* as well.

The existence of delayed implantation was hypothesized in pinnipeds as early as 1946 (Enders *et al.* 1946) in the Northern fur seal *C. ursinus*, which was confirmed subsequently by Pearson & Enders (1951). Numerous explanations for its presence have been forwarded, two of which are probably most important. Delayed implantation prolongs gestation, thereby increasing the survival of young animals by ensuring that they are born at an optimal season (Boyd 1991b). It also allows males and females to find separate feeding areas while still enabling them to converge on land/ice during the breeding season, which would be advantageous especially in animals where females exercise choice in mating

(York & Schaeffer 1997) even if non-migratory, such as the Cape fur seal (David 1987a), although probably of less importance in monogamous or serially monogamous species such as the crabeater seal (Le Boeuf 1986).

The current data set does not allow for establishing the precise timing of implantation in the Cape fur seal. All that can be stated unequivocally is that no animals had implanted by the end of March, while more than half of all animals which had ovulated, and would therefore be expected to implant a blastocyst (assuming, of course, successful mating and conception) had done so by the middle of April. It can thus be speculated, though with some confidence, that the median date of implantation would fall somewhere within April. This concurs with Rand (1955) who concluded that the average date of implantation may occur at, or before the middle of April.

Estimating the duration of delayed implantation requires an estimated date of parturition, which can only be speculated upon. Ovulation seems to occur from October (this study, Shaughnessy 1979) or even as early as September (Rand 1955) and continues into December, being concluded before the middle of January. While the present database may not be sufficiently representative to display the full range of implantation times (e.g. Rand (1955) observed embryos implanted as early as late March), and assuming a post-implantation gestation period of eight months (which seems to be the general rule in pinnipeds (Daniel 1981)), this study suggests a period of delayed implantation of at least 3 months. A median date of parturition of 1-4 December, observed by David (1987b) and Shaughnessy (1979), would give a period of delayed implantation of between 4-

4.5 months, assuming a week long post-partum, pre-ovulatory period. With the early commencement of ovulation in some animals, it is conceivable that the period of delayed implantation may last five months or longer. Such a duration is similar to the roughly four months observed by Rand (1955), and it falls within the 3-5 month range of delay common to otariids (Daniel 1981, Riedman 1990).

Numerous studies had been conducted on the factors affecting the timing of ovulation (e.g. Boyd 1991), especially the possible effect of photoperiod and hence latitudinal variation, and photoperiod has been found to in fact play a significant role both in mustelids, such as the spotted skunk (Mead 1981), European badger (Canivenc & Bonnin 1981), the stoat (Sandell 1984) and in pinnipeds, such as the Northern fur seal (Temte 1985, Daniel 1981, York & Scheffer 1997), the harbour seal (*Phoca vitulina*) (Temte 1994) and the Californian sea lion (Temte & Temte 1993). Furthermore, embryo reactivation occurs at a time of decreasing photoperiod (Boyd 1991b, Daniel 1981), possible exceptions being the harp seal which may implant during the period of maximum photoperiod (Daniel 1981) and the grey seal, where timing of implantation may be controlled indirectly by the temperature of the sea surface (Coulson 1981). Such a trend would fit in with the observed autumnal period of implantation observed in this study, although the available data does not allow any more specific conclusions. Since both serotonin and melatonin regulate reproductive processes as either a stimulator or a repressor of ovarian activity (Sirotkin & Schaeffer 1997), such photoperiodic control of the timing of implantation is entirely plausible.

The increase in follicular activity in the ovary with a CL prior to implantation (present study), coupled to the sharp drop in follicular activity thereafter, is strongly suggestive of a period of reduced luteal activity, followed by luteal reactivation. This has been suggested for the European badger (Mondain-Monval *et al.* 1980), Australian sea lion (Tedman 1991), ringed seal (Oritsland 1975), northern fur seal (Craig 1964, Yoshida *et al.* 1977, Yoshida *et al.* 1978), the subantarctic fur seal (Bester 1995) and the grey seal (Boyd 1983), a period called a false rut by Rand (1955) and Tedman (1991), coupled as it is, to oestrus behaviour outside the normal breeding season. A period of retarded luteal growth at this time is further suggested by the signs of luteal retrogression observed in cells during March, such as a clear, homogeneous cytoplasm, coupled to some degree of vacuolization. Similar signs of reduced luteal activity in the Northern fur seal has led Craig (1964) to suggest luteal inactivity during this period. This is supported by evidence for very low levels of luteal secretions prior to, followed by marked increases just before, during and after implantation in numerous species, such as the mink (Moller 1973a), European badger (Mondain-Monval 1980), the Antarctic fur seal (Boyd 1991a), the harbour seal (Reijnders 1990) and the northern fur seal (Daniel 1981).

The fact that both the overall size of the CL and the luteal cell sizes showed an increase from December/January to March may lead one to speculate that luteal inactivity during this period may not be complete and that some growth still occurs, as had been suggested for the Australian sea lion

(Tedman 1991), grey seals (Boyd 1984), harbour seals (Reijnders 1990) and ringed seals (Øritsland 1975).

Coupled to such similar trends in related species, it may be significant that, in comparing CLs of March / April, animals with implanted blastocysts in April had CLs which were significantly larger than CLs in (unimplanted) animals collected in March, while a much smaller difference in size between the two months was observed when using the CLs of April animals in which implantation had yet to occur (and thus, possibly, luteal reactivation as well). Confirmation of this can, however, only be done with hormonal evidence to back up morphological data.

The general cycle of luteal growth and regression up to parturition, and the follicular cycle observed during this time, appears to closely mirror that of other pinnipeds (Pike *et al.* 1960, Craig 1964, Yoshida 1978, Tedman 1991, Bester 1995). In *N. cinerea* in particular, Tedman (1991) reports luteal cells to be 15 μ m at 13-21 days post partum, peak at 40 μ m, and drop thereafter to 25-20 μ m and less while the overall size of the CL may increase to as much as 28 mm in size before regressing. This pattern is similar to that observed in the present study, where the average monthly luteal cells peaked at 36.4 μ m during August and the CL became as large as 26.7 mm during this time.

Craig (1964) reports that CLs in northern fur seals only peak at 15 mm, much smaller than in the Cape fur seal, but that cells reached 40-50 μ m in size, similar to what had been observed in the present study. Amoroso *et al.* (1965)

observed a CL of 17 mm in diameter in *H. grypus* with luteal cells 10-15 μ m in size during early pregnancy, increasing to 18mm and 30 μ m respectively just prior to parturition. Rand (1955) however, reports cells to reach 70 μ m during early pregnancy in the Cape fur seal, from a pre-implantation figure which may be 30-40 μ m, very much larger than that observed during this study, or in any pinnipeds for that matter. A possible explanation for this is not clear at present.

The post-partum persistence of the CA appears to show wide variation between species, disappearing within one year in *A. tropicalis* (Bester 1995), or are retained as long as 5-6 years post-partum in the crabeater seal (Bengtson & Siniff 1981), or even longer in the Australian sea lion (Tedman 1991). However, large numbers of CAs may have originated from double ovulations in mono-oestrus species (e.g. the grey seal, Boyd 1993) or even conceivably during polyoestrus cycles, as has been reported in the Hawaiian monk seal (Iwasa & Atkinson 1996) and which has not been discounted in the Australian sea lion (Tedman 1991).

Furthermore, variation within species in the retention of *corpora lutea* / *albicantia* may also be extreme, and CAs may disappear within one year post-partum (Pearson & Enders 1951), two years post-partum (Yoshida et al. 1978) or three years post-partum (Yoshida et al. 1977) in the northern fur seal. This variation in CA resorption, often coupled to the inability to unambiguously distinguish between CAs originating from single and double ovulations, makes any back calculations to previous years using only CAs highly dubious in the

Cape fur seal. However, when used in conjunction with placental scarring, determining the reproductive history to the previous year is entirely possible.

The general trend in pinnipeds is that placental scars remain visible for a year after parturition (e.g. Bengtson & Siniff 1981, Bester 1995). It could not be determined how long placental scars remain visible in the present study, due to the nature of the available material. It can be said that in the case of pregnancies to term, (or almost to term), such scars remain readily visible at least until the end of the following reproductive cycle (that is, roughly one year or more post-partum). They appear to disappear earlier in the case of abortions as has also been reported by Pike *et al.* 1960), and for this reason, missed pregnancies and abortions were not distinguished in this study, both being classed as prenatal mortalities. However, post-implantation abortions late in pregnancy may have been confused with pregnant cycles when calculating to the previous year using scars, but it has been assumed that the increased rate of resorption of CL observed in the case of abortions has made it possible to distinguish between the two. Even so, the incidence of reproductive failure may have been underestimated.

Reproductive studies of this sort often do not take into consideration the incidence of abortion, though it is generally reported that no pre-implantation differences can be observed between CLs of pregnancy and CLs of non-pregnancy (Pike *et al.* 1960, Craig 1964, Yoshida *et al.* 1978, Tedman 1991), and that CL regression in non-pregnant animals occur from the time that implantation would otherwise have occurred or, in the case of abortion, from the

time of the death of the foetus. Yoshida *et al.* (1978) in fact reports that any differences in CLs of pregnancy and of non-pregnancy can in fact only be observed about three months after implantation. Ouelette & Ronald (1985), on the other hand, suggest a possible slight advance in CL development in a pregnant animal over a non-pregnant animal, although such a difference, should it exist, would require knowledge beforehand of whether animals are in fact pregnant. Possibly a larger sample size would also be required.

The small monthly sample of abortions available in this study do not allow for any clear comparison with Yoshida *et al.* (1978) in this regard as neither of the May animals which have been classed non-pregnant can in fact unambiguously said to be such, while the single June abortion and both the July abortions are of a very recent nature, with little time since the presumed death of the conceptus for any significant luteal regression to have taken place. Observed differences in sizes observed during the first few post-implantation months may therefore be as likely be ascribed to actual luteal regression as to mere artifacts of small sample size. The extremely resorptive appearance of the CL of abortion in August (female 4070, roughly 4 months post-implantation), coupled to the excessively resorbed appearance of the CL of non-pregnancy in October and November (resorbed to the point of lacking all luteal cells, and consisting of a mass of CT and invading stromal tissue) suggests tentatively that resorption of CLs of non-pregnancy occur at least as fast in the Cape fur seal, and perhaps faster than in the northern fur seal (Yoshida *et al.* 1978). A stabilizing in regression rate appears to occur thereafter, so that placental scarring is required

towards the latter part of the following reproductive cycle to distinguish between successful and unsuccessful pregnancies from the previous year.

A functional CL tends to have a suppressive effect on follicular activity, both in otariids (this study, Rand 1955, Pike *et al.* 1960, Craig 1964, Yoshida *et al.* 1978, Bester 1995) and in Phocids (Øritsland 1975, Boyd 1983), and was noted as early as 1951 (Pearson & Enders 1951). Thus, ovulation alternates between ovaries over consecutive years, with the result that pinnipeds are generally mono-oestrus (Boyd 1991b) although both the southern elephant seal (*Mirounga leonina*) (Laws 1956) and the ringed seal (McLaren 1958) may follow an unconcepted ovulation with a second.

Possibly the only pinniped to be regularly polyoestrus is the Hawaiian monk seal (Iwasa & Atkinson 1996, 1997) although Tedman (1991) does not exclude a similar reproductive strategy in *N. cinerea*. Nevertheless, twinning does occur, albeit at a very low frequency (Harrison 1969, Spotte 1982). Bengtson & Siniff (1981) found evidence for a single case of twinning in *L. carcinophagus* and Bester & Kerley (1983) report a single case of twinning in *A. tropicalis*, while Rand (1955) found a frequency of twinning in the Cape fur seal (*A.p.pusillus*) of 3.5%, slightly higher than found in the present study.

By the qualification of Spotte (1982) (actual twin births or abortions being observed, or twin foetuses or embryos being found upon dissection), no positive evidence of twinning was found in this study. Since double ovulations need not necessarily result in double conceptions or implantations, the three cases of double ovulations found in this study only represent possible twinings. The

limitations of uterine horn material available for this study make it difficult to comment without speculation on this matter, but it can be said that at least one foetus had implanted in each of females 4147 and 5140, although no pregnancy to term had occurred in the former, and at least one had occurred in the latter. It may be significant that female 4147 had experienced a double ovulation during her first ovulation cycle, since the approach to first ovulation is one scenario whereby equal follicular activity in both ovaries can be expected to occur (e.g. Pike *et al.* 1960). The other two females found in this study with twin corpora have both ovulated in the same ovary, thereby removing the need for premature termination of pregnancy in the ovary with a CL. In cases where twin births do occur, however, survival to weaning of both seems to be very unlikely, one pup usually being rejected, and dying (Spotte 1982). This has been confirmed by observations by Rand (1955) in the Cape fur seal and Peterson & Reeder (1966) in the Northern fur seal. Instances have been recorded where females suckled two pups (eg. Bester 1983, Angot 1955), but assumptions that these pups are the result of twin births are not necessarily valid, since phocid females in particular may suckle another pup in addition to her own (Smith 1968). It has also be observed in the Cape fur seal that a yearling pup may continue to suckle into its' second year (David 1987b, Shaughnessy 1979). In such cases, "twin" pups would then represent offspring from consecutive years.

The Cape fur seal, rapidly increasing at an annual rate of 3% (Butterworth *et al.* 1995), is generally believed to be on the increase following extensive exploitation which was curbed by legislation only towards the end of the

nineteenth century. Whether or not the population has yet to reach its' pre-exploitation level is less certain. Data in this regard provide little evidence. David (1987b) reports a pregnancy rate of 0.74 for Cape fur seal females killed between 1956-1959, and 0.774 for females killed between 1975-1982. De Villiers *et al.* (1997) report a pregnancy rate of 0.85 for females at the Cape Cross breeding colony in the north of Namibia. The present study, using animals killed over a long period, but predominantly over the years around 1990, shows a pregnancy rate higher than that reported by De Villiers *et al.* (1997), but since they did not include abortions in their calculations, the birth rate in this study (Table 6) is probably a better estimate than the pregnancy rate for comparative purposes. This figure is slightly lower than that reported by De Villiers *et al.* (1997). This might be indicative of a slight increase in pregnancy rates over recent decades. Such a trend would indeed be suggestive of a population still to reach its pre-exploitation level, since the pregnancy rate would otherwise have been expected to decline.

The findings by de Villiers & Roux (1992) that new-born pups have a 20% mortality within the first 30 days post-partum may on the other hand be suggestive of density dependent effects caused by a population which is indeed approaching its' pre-exploitation level (Butterworth *et al.* 1995), even though the observations may not have been conducted over a suitably long time, or over a large enough area, to take into consideration the effects of short term geographic or temporal fluctuations. Additionally, obtaining pregnancy rates from females collected over several years may not take into consideration annual fluctuations

in for example food availability, and this may confound attempts to compare differences in pregnancy rates which do not differ all that much to begin with. Such interannual differences, as observed for the Antarctic fur seal (Boyd *et al.* 1995), Hawaiian monk seal (Johanos *et al.* 1994) and the South American fur seal (Lima & Paez 1995) may be inevitable in pinnipeds, and may result in substantial short-term fluctuations in reproductive aspects, but may have little influence on population dynamics in the long term.

A common feature in pinniped reproduction is the gradual increase in reproductive rates from a low early in life, peaking at some point, and then showing a decline thereafter as the females become older. Such an increase in reproductive rates from an initial minimum seems to be a common trend in fur seals, it having been observed in the Antarctic fur seal *A. gazella* (Lunn *et al.* 1994, Boyd *et al.* 1995), the northern fur seal (York & Hartley 1981), the south American fur seal *A. australis* (Lima & Paez 1995, 1997), the subantarctic fur seal (Bester 1995), as well as the and the Cape fur seal (this study). This study supports the former trend, that of increased reproductive rate with increasing age, from a low of 0.17 at age three, rapidly increasing to 0.71 at age four, peaking at age six and remaining high thereafter. It has to be emphasized that the total sample size ($n = 83$) is in all likelihood insufficient to calculate such a variable population attribute as age-specific pregnancy rate, hence the erratic appearance observed in Fig. 41. The sudden and inexplicable drops observed in the five, seven and eight year old groups may simply represent an artifact of small sample size.

An increase in reproductive rates also appears to be common in phocids, such as the crabeater seal (Bengtson & Siniff 1981), the harbour seal (Bjørge 1992), the Kuril seal (*Phoca vitulina stejnegeri*) (Hayama et al. 1986) and the ringed seal (Øritsland 1975), all of which show low initial rates of fecundity, often because of a high rate of abortions during early post-pubertal reproductive cycles, followed by a reproductive peak from about six years of age. Possibly this is common, although reproductive studies often do not distinguish between age at puberty and age at sexual maturity, sexual maturity often being given as the age at which *corpora lutea/albicantia* or mature follicles are first observed. Early in life, females may fail to successfully bear young not necessarily because of reproductive immaturity, but rather because of their investing maximal resources into growth, with little remaining to support a foetus, resulting in a high proportion of reproductive failures. This may be reflected in the differences between the average age of puberty and the average age of sexual maturity observed in the present study.

The older age group (13 yrs +) observed in this study still has a very high rate of reproduction of 0.87, which - considering the relatively large sample (n = 23) - does not suggest any reproductive senescence at this age. The female Cape fur seal may, however, reach and even far exceed twenty years of age (Wickens 1993), so that the 13+ year age class may have included both older, (and possibly reproductively failing) females along with relatively younger and possibly still vital females. Reproductive senescence may be the rule in fur seals, as it has been observed in the Antarctic fur seal *A. gazella* (Lunn et al. 1994,

Boyd *et al.* 1995), the northern fur seal (York & Hartley 1981), the South American fur seal *A. australis* (Lima & Paez 1995, 1997) and the subantarctic fur seal (Bester 1995). Boyd *et al.* (1995) suggests, however, such a lowered fecundity in older females to be the expression of the large cost in survival to females who breed, and that older females reach their older age by virtue of their having had low reproductive rates throughout their lives, more fecund animals having died young.

Undoubtedly there are certain areas in this study which demand attention. In particular, in calculating the average age at sexual maturity or the age-specific pregnancy rates, the relatively small sample size of known-age females can not give the accuracy which is required for such vital population attributes. As more ages for females used in the present study become available, the sample size can then be increased. Increasing the sample size in this manner, however, will introduce other errors. All known-age animals were collected over a very few years and were collected opportunistically and at sea. The females of unknown age were for the most part collected much more recently (1997/1998) and were all collected on land. This may introduce temporal variation in age-specific population attributes, and will not take into consideration the possible errors in comparing pregnancy rates of females collected on land, and females collected at sea.

Nevertheless, this study has provided some information in estimating population characteristics in quantitative terms, and has provided an account of the annual reproductive cycle of the Cape fur seal. With increased sample sizes

and the standardization in the collection and the subsequent processing of material, this study can be expanded upon to provide more accurate information on the population characteristics of the Cape fur seal for management or conservation purposes.

Chapter 5: Conclusions

This study is not the first to examine either the annual reproductive cycle, or the reproductive population characteristics of the female Cape fur seal. It is, however, as far as could be ascertained, the first to combine a histological description of the reproductive cycle with a reliable technique for age determination. It has also provided information on the reproductive history of 159 females, and has enabled the age at puberty, the age at sexual maturity, overall pregnancy rates and the age-specific pregnancy rates to be calculated using a sub-sample ($n = 83$) of these. Information of this nature is valuable from the point of view of obtaining a fuller, qualitative understanding of the biology of the species, especially in light of the conflicts between the growing seal population and the fisheries industry.

It has to be emphasized, however, that considerable errors have occurred in this study which will have to be addressed, should this study be expanded upon in future. Firstly, there has to be standardization in the treatment of material. Examination of the uterine horns, looking for evidence of placental scarring and hence, positive proof of pregnancy, is a relatively quick and easy, yet invaluable component of a study of reproductive organs. It is therefore advisable to collect both complete uterine horns, and store each with its relevant ovary, rather than a sample of each. This will also allow one to – if necessary – flush the uterine horns at a later stage in looking for unimplanted blastocysts during the pre-implantation months. Alternatively, a single person could be responsible for both the collection and the examination of the material, in which

case the material can be examined in the field, although reduced accuracy might result from this. Availability of the entire uterine horn would remove the necessity of applying the dubious technique of inferring pregnancy based on CL/CA appearance alone, where size variation between individuals might lead to borderline cases being misinterpreted.

This study has also identified the need on occasion to verify ovarian structures histologically. In particular, the presence, appearance, shape and size of luteal cells may assist in distinguishing between CLs of pregnancy and of abortion, and may also assist in distinguishing between very old CAs and *corpora atretica*. Preserving material by freezing rather than using a chemical fixative makes such an exercise more difficult, or, at worst, impossible. This aspect should be taken into consideration when preserving material.

Finally, in collecting material for a study on the annual reproductive cycle, a sample for each month of the year is of necessity required. This is, however, not ideal for the calculation of pregnancy rates, where it would be better to obtain a single, large sample of animals during a short period at about 3-4 months post-implantation. This will allow non-pregnant animals to be distinguished from pregnant animals with a very high degree of confidence, since the regressed appearance of the *corpora lutea* (as compared to gravid corpora) and the absence of placental scars would be distinctive in these animals.